University of Venda
Creating Future Leaders

INVESTIGATION OF THE COVARIABILITY BETWEEN ENERGY FLUXES AND CO_2 EXCHANGE OVER A SEMI-ARID SAVANNA (KRUGER NATIONAL PARK) BY EDDY COVARIANCE TECHNIQUE.

BY

TAKALANI LUFUNO

(11570116)

DISSERTATION

PRESENTED IN PARTIAL FULFILMENT FOR THE REQUIREMENTS OF THE MASTER OF SCIENCE (M.Sc.) DEGREE

IN

PHYSICS

FACULTY OF SCIENCE, ENGINEERING, AND AGRICULTURE

AT THE

UNIVERSITY OF VENDA

SUPERVISOR: DR. T.S. MULAUDZI (UNIVEN)

CO-SUPERVISOR: PROF. N.E. MALUTA (UNIVEN) AND DR. M. MATEYISI (CSIR)

Ms. H THENGA (CSIR)

YEAR: 2023

DECLARATIONS

I, Takalani Lufuno (11570116), hereby declare that this dissertation titled “Investigation of the covariability between energy fluxes and CO_2 flux exchange at Skukuza (Kruger National Park) by Eddy Covariance technique” is my original work and has not been submitted for any degree at any other university or institution. The dissertation does not contain another person’s writing unless specifically acknowledged and referenced accordingly.

Signed by _____ at University of Venda

Date: 14 August 2023

DEDICATIONS

This dissertation is dedicated to my beloved wife Vhutali Nyeleti Takalani, my sons, Muhulu and Mukonazwothe Takalani, and not forgetting my parents and siblings for their support.

ACKNOWLEDGEMENT

I want to thank God for enabling me to write this dissertation and strengthening me throughout the whole study. I would also extend my gratitude to my supervisor Dr. T.S Mulaudzi and co-supervisor, Prof. N.E Maluta, Dr. M Mateyisi, and Ms. H Thenga for helping me throughout this research with the assistance of the data from Council of Scientific and Industrial Research (CSIR). I extend my utmost gratitude to the Faculty of Science, Engineering, and Agriculture at the University of Venda, especially the Department of Physics, for the opportunity to proceed with the master's degree. I want to thank my colleagues Mr. TS Ranwaha, Mr. TT Khedzi, and others for their support. I am also thankful for the student grant from Thunen Institute that supported me financially.

ABSTRACT

South Africa faces climate change, natural disasters, and rising temperatures due to increased levels of carbon dioxide in the atmosphere, primarily caused by deforestation, burning fossil fuels, and releasing carbon dioxide into the atmosphere without additional carbon sinks. The gap in understanding lies in studying the connection between energy flows and Net Ecosystem Exchange (NEE) at the semi-arid savanna of Kruger National Park to gain a more detailed and accurate understanding of these processes, especially in semi-arid savannas that are susceptible to changes in environmental factors. By studying energy fluxes and NEE at Kruger National Park using the eddy covariance technique, the dissertation seeks to deepen our understanding of the mechanisms driving carbon exchange in semi-arid savannas and provide insights into the impact of environmental factors on ecosystem processes. The eddy covariance technique is a powerful tool that directly measures energy and carbon dioxide exchange between the land surface and the atmosphere. The study shows that the correlation between NEE and latent heat flux (LE) and net radiation (Rn) is generally the strongest, while ground heat flux (G) and sensible heat flux (H) have little impact on NEE. The dataset provides insight into the biometeorological and flow dynamics of the Skukuza ecosystem and how it responds to climate change. The study emphasizes the importance of considering seasonality, climatic variability, and precipitation when studying the surface energy balance and its components. The findings have implications for understanding the complex interactions between ecosystem processes and environmental factors.

Keywords: Carbon dioxide, energy fluxes, eddy covariance, net ecosystem exchange

TABLE OF CONTENTS

LIST OF FIGURES

LIST OF TABLES

LIST OF ABBREVIATIONS

ANN	-	Artificial Neural Network
CO_2-m	-	CO_2 mixing ratio.
EC	-	Eddy Covariance
ET	-	Evapotranspiration
G	-	Soil heat flux
GPP	-	Gross Primary Production
KNP	-	Kruger National Park
Lwin	-	Incoming Longwave radiation
Lwout	-	Outgoing Longwave radiation
Rn	-	Net Radiation
PAR	-	Photosynthetically Active Radiation
QA/QC	-	Quality Assurance/Quality Control
Fc	-	CO_2 flux, sometimes referred to as.
NEE	-	Net ecosystem exchange
MOD16	-	Moderate Resolution Imaging Spectroradiometer
H	-	Sensible heat
ISLSCP	-	International Satellite Land Surface Climatology Project
FIFE	-	Field Experiment
λE/LE	-	Latent heat
RH	-	Relative humidity
SEB	-	Surface Energy Balance
Swin/Rg	-	Incoming Shortwave radiation/global
Swout/Rr	-	Outgoing Shortwave radiation/reflected.
Ta	-	Air Temperature
Ustar	-	Frictional velocity
VPD	-	Vapor Pressure Deficit
wd	-	Wind direction
WPL	-	Webb Pearman Leuning
ws	-	Average wind speed

CHAPTER ONE

1. Introduction

1.1. Background

The modern world struggles with climate change, natural disasters, and rising temperatures. The amount of CO_2 in the atmosphere is at its most significant level in at least 800,000 years (IPCC, 2021). Deforestation, burning fossil fuels, and releasing carbon dioxide into the atmosphere without additional carbon sinks can be the primary causes of these changes. Understanding the connection between the fluxes will be aided by researching the relationship between energy flows and the Net Ecosystem Exchange (NEE) at the semi-arid savanna of Kruger National Park. Semi-arid savannas are ecosystems that are more susceptible to changes in environmental factors, such as temperature and precipitation. The study can be used to better comprehend this type of ecosystem by looking at how energy fluxes and NEE interact. NEE is a measure of the difference between an ecosystem's CO_2 uptake (photosynthesis) and CO_2 release (respiration) over a specific time frame.

Using the eddy covariance approach to look into the covariability between energy flows and Net Ecosystem Exchange (NEE) at the semi-arid savanna Kruger National Park, we can bridge gaps in our understanding of ecosystem processes. The eddy covariance technique is a powerful tool for determining the direct energy and carbon dioxide exchanges between the ground surface and the atmosphere. By using this method to examine the connection between energy fluxes and NEE at Kruger National Park, we may gain a more thorough understanding of these processes than is achievable with other methods. We may use the eddy covariance approach to gain a better understanding of the mechanisms driving carbon exchange in these ecosystems, as semi-arid savannas are significant habitats for carbon cycling due to their size.

The study sheds light on the effects of climatic variables on ecosystem processes, including how temperature and precipitation affect carbon uptake and release in semi-arid savannas. Additionally, it improves the researcher's capacity to estimate and forecast adjustments to ecosystem functioning and carbon exchange in semi-arid savannas under various future climatic scenarios. It will give a more thorough understanding of the part played by semi-arid savannas in the global carbon cycle and the possible effects on the climate of changes to these ecosystems. Using the eddy covariance approach, research on the relationship between energy fluxes and NEE at the semi-arid savanna Kruger National Park can offer crucial insights into ecosystem processes, carbon cycling, and the effects of environmental change on these systems.

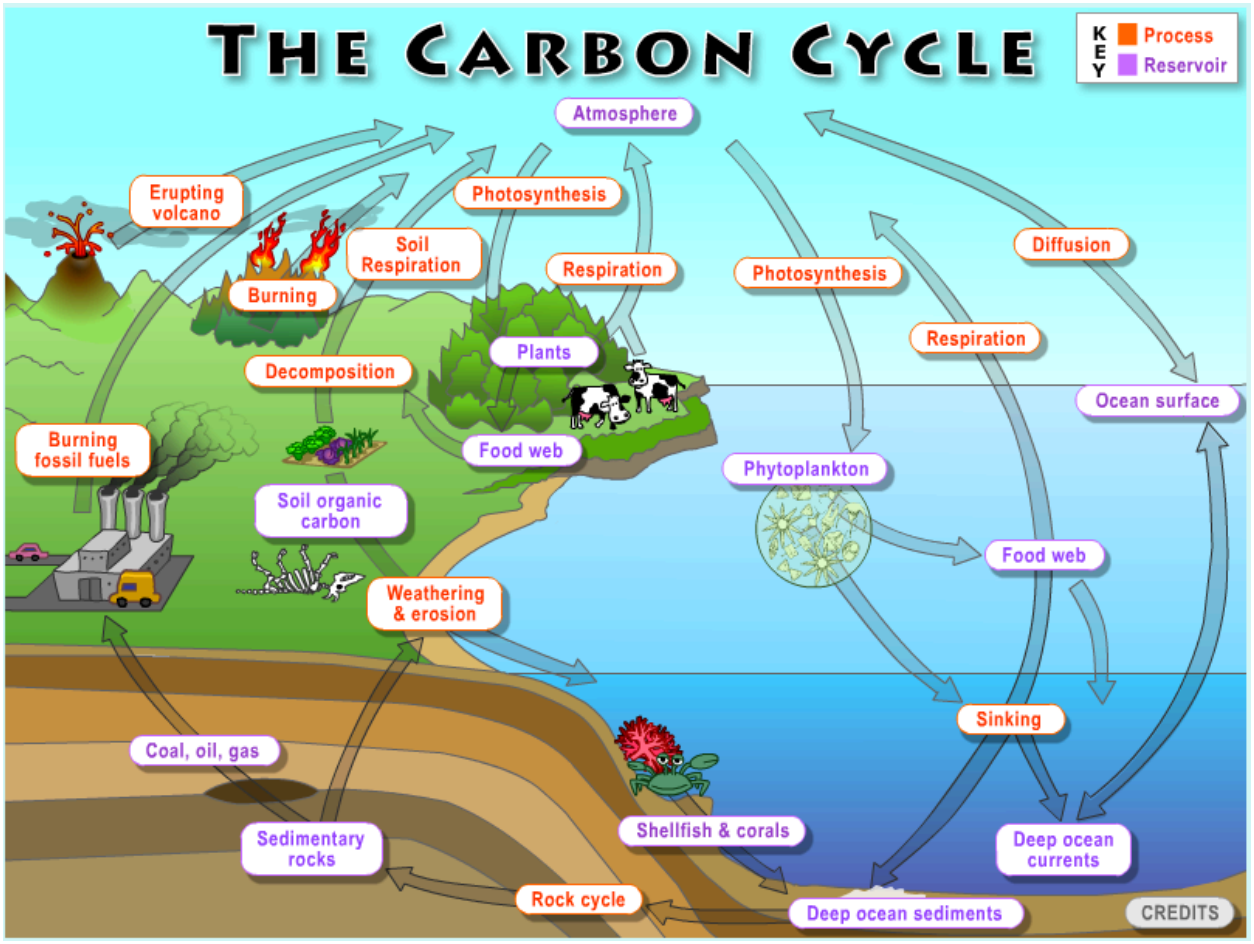

Figure 1.1. The Carbon Cycle from the Earth labs *(Lab Overviews (carleton.edu)*

Figure 1.1. Explore the role of food webs within the natural carbon cycle by tracking a carbon atom through forest reservoirs, focusing on photosynthesis, respiration, and decomposition.

1.2. The Eddy Covariance method

1.2.1. The method background.

The Eddy Covariance method is a statistical technique used in meteorology and other fields like micrometeorology, oceanography, hydrology, sciences, and industrial and regulatory applications to calculate the exchange rates of trace gases over natural ecosystems and agricultural fields and the rates of gas emissions from land and water areas. It is commonly employed to calculate the fluxes of momentum, heat, water vapor, carbon dioxide, and methane*(Baldocchi, D et al. 1988, Verma, S.B.et al.1990, Lee, X.et al. 2004, Burba, G. et al. 2013, Aubinet, M. et al. 2012).*

The method is also widely used for validating and fine-tuning regional weather forecasts, complicated biogeochemical ecological models, and satellite and aircraft-based remote sensing estimates. The method requires meticulous setup and data processing and involves complex mathematics. Although the Eddy Covariance technique does not currently have a standard vocabulary or methodology, flux measurement networks like FluxNet, Ameriflux, ICOS, CarboEurope, Fluxnet Canada, OzFlux, NEON, and iLEAPS are working hard to bring the diverse methods together.

1.2.2. The system operation and data acquisition instruments

In contrast to meteorological measurements, which began in February 2000, the study uses an Eddy Covariance system that was built close to Skukuza Camp in the Kruger National Park, South Africa. The first flux measurements were made in April 2000. Due to issues with operation and upkeep, hydro-ecological years were used in this study.

Since the micrometeorological apparatus is positioned on a tower in the savanna with broad-leaved Combretum and fine-leaved Acacia trees, the location is noteworthy. With a 30-minute average time, wind patterns enable the collection of a high-quality sample of net ecosystem flows of CO_2, water, and energy as well as measurements of numerous meteorological variables.

Additional continuous data for the savanna system include the soil heat flux, soil temperature, and soil moisture (from the soil surface to the bedrock), as well as the oxygen concentration, humidity, and air temperature in the canopy. Intermittent measurements involve soil surface CO_2 flux in addition to other, regionally distributed measurements of soil moisture and soil temperature*(Scholes, R et al. 2001).*

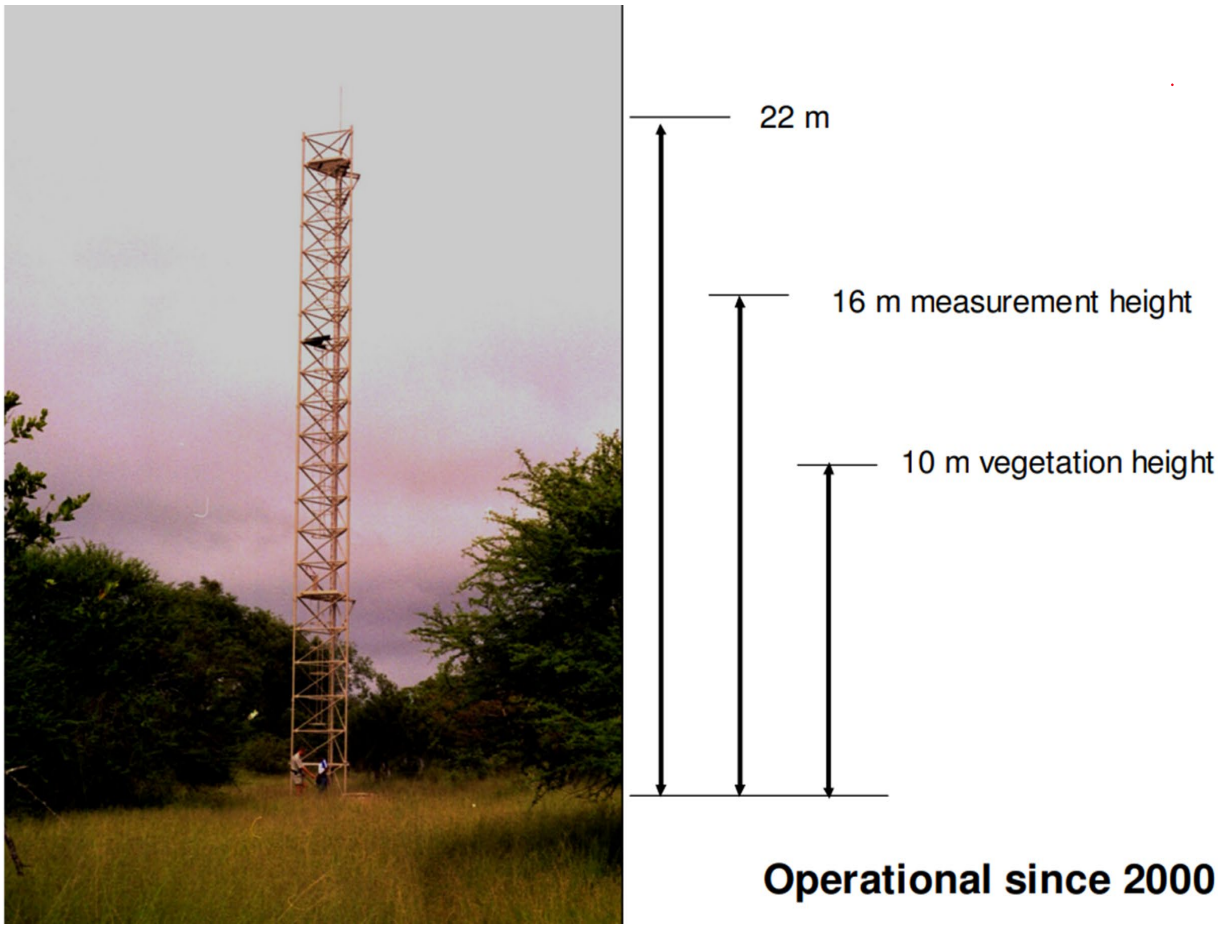

Figure 1.2. The Skukuza Eddy flux tower(*RJ Scholes,* Archibald, and A Nickless *2010*).

The LI-7500 Open-path system is used in the investigation and provides accurate, reliable, and low-maintenance measurements. The system is perfect for long-term research at remote locations because of its outstanding frequency response and low power requirements. Open-path instruments cannot be protected from numerous impacts because of the nature of their design, especially when there is a lot of dust, water, or ice.

Table 1.1: Currently operational long-term Eddy Covariance flux towers in South Africa (https://www.csir.co.za/eddy-covariance-flux-towers)

Name	**Location**	**Operational since**	**Approach**	**Operated/ established by**
Skukuza	-25.02°, 31.49°	2000	Savanna/conservation area	CSIR
Malopeni	-23.83°,31.21°;	2008	Savanna/conservation area	CSIR
Welgegund	-26.56°,26.93°;	2010	Grassland / commercial agriculture	North-West University
Cathedral Peak	-28.98°, 29.24°	2012	High-altitude grassland	SAEON
Middelburg (1 and 2)	-31.52°, 25.01°	2015	Nama Karoo / paired setup, heavy and lenient grazing	GADI/EMSAfrica through Thünen Institute
Agincourt	-24.82°, 31.21°	2016	Savanna / communal area	CSIR
Vuwani	-23.14°, 30.43°	2016	Savanna / communal area	University of Venda/EMSAfrica through

				Thünen Institute
Benfontein Savanna	-28.89°, 24.86°	2020	Kimberly Thornveld, paired setup, the transition from Savanna-like to Nama-Karoo-like vegetation	SAEON
Benfontein Nama-Karoo	-28.86°, 24.84°	2020	Kimberly Thornveld, paired setup, the transition from Savanna-like to Nama-Karoo-like vegetation	SAEON

1.3. Purpose of the study

1.3.1. Aim

In this study, we aimed at investigating the covariability between energy fluxes and CO_2 flux exchange at Skukuza (Kruger National Park) using the Eddy covariance technique.

1.3.2. Objectives of the research

Objective 1: Characterize the patterns of energy fluxes and net ecosystem exchange at various temporal scales. This objective involves analyzing the diurnal patterns of energy fluxes across different seasons and inter-annual variability. To achieve this objective, we conducted a time series analysis, regression models, and integrated meteorological parameters to identify drivers of CO_2 exchange and energy flux.

Objective 2: To establish a covaribility between CO_2 flow statistics and energy fluxes, as well as to pinpoint the mechanisms responsible for variations in net ecosystem exchange. To accomplish this goal, we investigated the relationships between CO_2 flow and energy flux characteristics using correlation analysis and regression models.

Objective 3: To investigate energy balance closure and its relationship with CO_2 flux. We investigated the relationship between energy balance closure and CO_2 flux, explored the diurnal variation of closure, and identified the patterns and closure residuals and CO_2 exchange.

CHAPTER TWO

2. Literature review

2.1. Drivers of Net Ecosystem Exchange (NEE)

The eddy covariance method is a powerful technique for the quantification of CO_2, H_2O, and energy fluxes in natural ecosystems. The technique is applied at Skukuza Kruger National Park to assess the ecosystem's energy fluxes and net ecosystem exchange (NEE). The study can show how an ecosystem is responding to environmental changes by monitoring the NEE and energy fluxes, which are two variables that a variety of factors can influence. The following important factors could be examined at Skukuza Kruger National Park using the eddy covariance method:

(a) Temperature: The rates of photosynthesis and respiration in plants can be directly impacted by temperature, which can therefore impact NEE. Elevated temperatures can also speed up evapotranspiration, which can impact energy fluxes.

(b) Water availability can impact the rate of photosynthesis and respiration

(c) Solar radiation: Solar radiation is a significant catalyst for photosynthesis and has an impact on energy flows as well as NEE. The rate of evapotranspiration and the surface temperature can be impacted by solar radiation.

(d) Wind direction and speed: These factors can impact the flow of heat, moisture, and gases, as well as the rates of photosynthesis, respiration, and energy fluxes.

(e) Changes in atmospheric CO_2 concentration can directly impact NEE because they can alter the rates of photosynthesis and respiration.

By measuring the fluxes of carbon dioxide and energy using the eddy covariance technique and investigating how these fluxes vary in response to changes in these drivers, research can gain insights into the functioning of the ecosystem and how it is responding to environmental changes.

Three co-located eddy covariance (EC) tower data, hyperspectral aircraft images, footprint analysis, and data from the three EC systems were used to analyze regional flux fluctuation within a savanna-like ecosystem in central Spain. Sensible heat (H) was shown to be negatively correlated with surface temperature for both individual towers and for differences between towers over time, indicating that higher H was seen at lower surface temperatures. The higher aerodynamic conductance of tree canopies lowers the canopy surface temperature, and the excess energy is released as H. Therefore, higher H was seen at colder surface temperatures. Latent heat (LE) flow variations between towers did not always correspond to the vegetation index.

Most likely, soil's substantial contribution to this missing association is to blame. None of the biophysical or structural aspects of the ecosystem can explain ecosystem LE evaporation. Three different metrics of uncertainty, including the standard deviation of the marginal distribution sampling (MDS), the two-tower approach (TTA), and the variance of the covariance (RE), were looked at to determine whether geographic heterogeneity affected the uncertainty of the observed fluxes. Despite the fact that the three techniques were very different from one another, the three uncertainty estimates at each tower had comparable means and distributions *(T.S. El-Madany et al.2018).*

An important study conducted in Kaziranga National Park discovered that because of their function in photosynthesis, the Leaf area index (LAI) and its variations are important drivers of CO_2 and H_2O exchange in a forest ecosystem. The study tracks the seasonal variations in CO_2 and energy fluxes in a semi-evergreen primary forest inside Kaziranga National Park in Assam, India, between February 2016 and January 2017. It was revealed that the half-hourly average CO_2 fluxes over the diurnal pattern of the forest are mostly regulated by incident photosynthetically active sunlight. The CO_2 flux varied during the day, reaching its maximum in June, when the monsoon season began during the research period, at 9.97 mol m^{-2} s^{-1} *(Dipankar Sarma et al. 2018).*

2.2. Greenhouse gases, their warming effect, vegetation production in terrestrial ecosystems, and evapotranspiration

Fluxes of greenhouse gases from vegetation and agricultural fields can be measured by eddy covariance as referenced in micrometeorology. Vegetation production can be monitored using eddy covariance technology in conjunction with nutrient supply information by monitoring net CO_2 and H_2O fluxes. Readings can be taken from flux towers over several years to determine water use efficiency among others (Schlesinger, William H.et al., 2013). Measuring the vertical turbulent flux of gas states of H_2O, CO_2, heat, and CH_4, among other volatile organic compounds monitoring equipment, can be used to infer canopy interaction. Landscape-wide interpretations can then be inferred using gathered data. High operational costs, weather limitations (some equipment is better suited for certain climates), and their resulting technical limitations may limit measurement accuracy *(Jalota, S. K.et al.2018).*

Vegetation production models require accurate ground observations from eddy covariant flux measurement in this context. Eddy covariance is used to measure the net primary production and gross primary production of plant populations. Advancements in technology have allowed for minor fluctuations resulting in a scale of 100–2000-meter measurements of air mass and energy readings. Studying the carbon cycle on vegetative growth and production is important to both growers and scientists. Using such information, carbon flux between ecosystems and the atmosphere can be observed, with applications ranging from climate change to weather models *(Liang X; et al. 2012).*

Remote sensing is another approach for modeling evapotranspiration using an energy balance and the latent heat flux to find evapotranspiration rates. Evapotranspiration (ET) is a part of the water cycle, and accurate ET readings are essential to local and global models to manage water resources. ET rates are an important part of research in hydrology-related fields, as well as for farming practices. MOD16 is an example of a program that measures ET best for temperate climates *(Liang, et al. 2012, Jia, L.; et al.2018).*

2.3. CO_2 flux exchange

Significant research on the CO_2 fluxes was carried out by *Morales-Rincon et al. 2021*, who stated that agriculture was being quickly introduced to the natural savannas of the Orinoco River basin ("Llanos") in Colombia. It needed to be clarified how this transition might affect CO_2 flows and build-up to comprehend the carbon cycle and underlying mechanisms of the ecological services provided by the Llanos natural savanna. In the study, assessments of two years of carbon dioxide flux observations were presented. During the measurement period, climatic conditions, notably rainfall, were highly variable.

The savanna had a modest carbon supply (35 gCm^{-2}) in the first year of data, but a large carbon sink (273 gC m^{-2}) was present in the system in the second year, despite having less rainfall. As anticipated, the amount of water in the soil, ecosystem respiration, and global solar radiation all had a significant impact on the savanna's net ecosystem exchange (NEE). It was shown that the NEE was highly dependent on the length of the nominal drought, which is defined as less than 5 mm/day of precipitation, after about 10 days. After around 60 days of nominal dryness, the ecosystem reached a crucial point where photosynthetic activity began to decline. A straightforward, traditional meteorology-based model was used as a result of these discoveries, and it was able to accurately match the data. The outcomes show a change *(Luis A. Morales-Rincon, Andrea J. Hernandez, Nubia S. Rodriguez-Hernandez, and Rodrigo Jimenez, et al. 2021).*

Three different types of models were taken into consideration in a study that sought to model carbon fluxes for a karst grassland in Slovenia: (1) a linear relationship between Gross Primary Production (GPP) and each vegetation index; (2) a linear relationship between GPP and the product of a vegetation index with photosynthetically active radiation; and (3) a simplified LUE (Light Use-Efficiency) model assuming a constant LUE. Three accuracy metrics—the coefficient of determination (R2), the root means square error (RMSE), and the Akaike Information Criterion were used to determine the performance of several vegetation indicators collected from two remote platforms (Landsat and Proba-V) *(Noumonvi et al. 2019).*

Li X, Liu L, Yang H, Li Y, et al. (2018) studied the effects of environmental conditions and human activity on agricultural emissions and carbon fixing. We investigated the correlations between carbon fluxes and environmental variables in a drip-irrigated, film-mulched cotton crop in Wulanwusu, northern Xinjiang, an arid region of Northwest China. The study found that cotton fields with plastic film mulching and drip irrigation had a cumulative net carbon flow (NEE) for the entire growing season of 2012 that was higher at -304.8 g C m^{-2} (a significant sink). The correlations between gross primary productivity (GPP), air temperature (Tair), net solar radiation (Rn), and soil water content (SWC) also changed as the time scale increased from a half-hour to a year.

The energy and carbon dioxide fluxes in four different habitats in the Pallas region of northern Finland, the Kenttärova spruce forest, the open Lompolojänkkä wetland, the treeless top of Sammaltunturi fell, and Pallasjärvi, a lake, were assessed using the eddy covariance method in yet another critical study by *Aurela M. et al. (2015).* It was found that the short-term fluxes and long-term balances of carbon and energy in these ecosystems differed. Between the sites, there were considerable differences in the amount of solar energy that was available and how it was divided into sensible and latent heat fluxes.

Regarding maximum uptake and emission capacities and the corresponding reactions to environmental variables, the CO_2 exchange characteristics at different sites varied. The marshes and woodlands have the highest instantaneous fluxes. While the forest balances were very close to zero, the mean annual balance at the wetland showed a significant net intake. On the other hand, it was believed that the lake was a sizable source of carbon dioxide. The significance of adding all the critical ecosystems in the landscape CO_2 balance was highlighted by an upscaling experiment based on the actual land-use map of the immediate area.

Another significant study on carbon dioxide fluxes by Quansah E. et al. was completed in 2015. They conducted their research in three separate locations within the West African Sudanian Savanna. They found that throughout the dry season (November to March), poor soil moisture availability, a sizable vapor pressure deficit, and reduced ecosystem respiration were frequent occurrences. Net carbon outflow occurred during the dry season as well as the dry-to-wet and wet-to-dry transition periods. On the other hand, individuals consumed the most carbon during the wet season. Grassland, fallow land, and agricultural land all experienced a decline in the quantity of carbon they absorbed. Due mostly to the ecosystem's use of water, only the ecology of Burkina Faso's Nazinga Park natural reserve functioned as a net CO_2 sink.

Local evapotranspiration (ET) has been identified in several South African situations. Due to a lack of suitable tools, accurate spatially exact information on ET is difficult to come by across the nation. In 2014, Ramoelo A. et al. created a remote sensing ET product from the Moderate Resolution Imaging Spectrometer (MOD16). Sadly, ecologists in South Africa were unaware of its veracity. The MOD16 ET product was tested in this study using information from the Skukuza and Malopeni eddy covariance flux towers, which were built in a savanna and woodland ecosystem in the Kruger National Park, South Africa. To match the eight-day cumulative ET data from the flux towers, eight-day MOD16 products were created *(Ramoelo A.et al. 2014).*

Due to a shorter measurement period and a poorer MOD16 ET comparison at the Malopeni site than at the Skukuza, only the 2009 results were validated. Among other factors, flux tower measurement issues, parameterization of the Penman-Monteith model, and comparison of the flux tower footprint to the open access Modis pixel were blamed for the inaccurate comparison of MOD16 with flux tower-based ET. For application in South Africa's integrated water management, a locally parameterized and updated solution was proposed. MOD16 is crucial for making worldwide conclusions concerning ET.

Notably, *Bombelli et al. 2009* demonstrated that Sub-Saharan Africa's (SSA) forest net carbon balance was almost at equilibrium and that the impact of forest degradation was greater than that caused by deforestation. Savannas have a big impact on the carbon balance in the SSA due to their large area, risk of fire, and considerable interannual NEP variability. But they also significantly increase the budget's overall risk. According to this research, Africa is an important player in the global carbon cycle system and may have a greater capacity for carbon sequestration than previously believed. To fully comprehend the purpose of savannas and tropical forests, more research is necessary. The current CarboAfrica carbon measurement network could provide unique data sets for more precise calculations of the carbon balance in Africa.

The interannual variability in primary output and ecosystem respiration was examined by Archibald et al. (2008) using eddy-covariance data from a semi-arid savanna area in Kruger Park, South Africa. The study created brand-new techniques in semi-arid environments for filling in data gaps in eddy-covariance studies and extending overnight respiration to the full day. Since rainfall events were the primary triggers for pulses of net ecosystem exchange (NEE) in these systems, the majority of the existing conventional gap-filling techniques were created for regions with temperate flux. Additionally, it should have been considered that respiration decreases at high soil temperatures. With a mean absolute error (MAE) of only 0.42 gC/m^{-2}/day, an artificial neural network (ANN) model using these features was able to predict the site's seasonal patterns of photosynthesis and respiration.

The study developed new methods for filling in eddy-covariance data in semi-arid settings and daily projection of nighttime respiration. Traditional gap-filling strategies were largely developed for places with temperate flux, despite the fact that these systems saw pulses of net ecosystem exchange (NEE) associated with rainfall events. It should also have considered how respiration decreased at high soil temperatures. An artificial neural network (ANN) model employing these features could predict the site's seasonal patterns of photosynthesis and respiration with an accuracy of just 0.42 gC/m^{-2}/day.

2.4. Flux corrections

Flux corrections are used in the eddy covariance technique to take into account the impacts of numerous variables that may have an impact on the observed fluxes. To guarantee that the fluxes accurately depict the exchange of energy and gases between the atmosphere and the underlying surface, several modifications are required. These consist of:

(a) Attenuation correction: This correction is applied to account for the reduction in turbulence intensity with height above the ground. The attenuation correction factor is typically determined by fitting a power-law function to the vertical wind speed profile.

(b) Spectral correction: This correction accounts for the loss of turbulent energy at high frequencies due to instrument noise and filtering. The spectral correction factor is typically determined by comparing the high-frequency part of the turbulent spectra with theoretical models.

(c) Coordinate rotation: This correction is applied to align the coordinate system of the anemometer with the horizontal plane. This correction is necessary because the wind direction measured by the anemometer is not necessarily aligned with the horizontal plane.

(d) WPL correction: Webb, Pearman, and Leuning (WPL) correction is applied to account for the effects of density fluctuations on the measured fluxes. This correction assumes that the density fluctuations are proportional to the water vapor fluctuations.

(e) Time lag correction: This correction accounts for the time delay between the measured turbulent fluxes and the corresponding atmospheric variables. The time lag is typically determined by cross-correlating the turbulent fluxes with the atmospheric variables.

The Webb adjustment was initially used to correct water vapor fluxes and is now known as the WPL correction after its developers, Webb, Pearman, and Leuning (1980). They extended its application to the measurement of eddy fluxes of trace gases. Following Webb et al.'s (1980) publication, numerous authors investigated this topic, as detailed by Liebethal and Foken (2003, 2004), Fuehrer and Friehe (2002, 2002), Lee and Massman (2011, 2012), and Fuehrer and Friehe (2002, 2002). These authors reached similar conclusions but proposed different solutions (Liu 2005). The issue was recently described by Leuning (2004, 2007).

2.5. Energy closure problem

When the measured energy fluxes such as latent heat, sensible heat, and ground heat flux do not balance out with the available energy, which is calculated as the net radiation (incoming solar radiation minus outgoing longwave radiation plus the storage heat flux in the ecosystem), there is an issue known as the energy closure problem in eddy covariance. Several variables, including measurement errors, instrument calibration, and uncertainty in estimating the available energy can cause the energy closure issue in eddy covariance measurements. The imbalance may also be influenced by unmeasured energy fluxes, such as heat advection, not considered in the eddy covariance measurements.

There are numerous ways to deal with the energy closure issue in eddy covariance measurements. These include enhancing measuring methods and instrument calibration, performing quality assurance checks, and considering unmeasured energy fluxes by supplementary measurements or modeling. To precisely quantify the flow of energy and gases between ecosystems and the atmosphere, which is essential for comprehending and foreseeing the effects of climate change on Earth's ecosystems, the energy closure problem in eddy covariance measurements must be solved.

When eddy covariance (EC) readings were compared to Bowen-ratio measurements, which close the energy balance, the first signs of an open energy balance were clear. Studies conducted in June in the three years that followed, 1982, 1983, and 1984, as well as in Australia in 1981, produced similar findings (Leuning et al.1982). 1988; Koitzsch and others. In Kursk, Russia, during an experiment in 1988, a non-closed energy balance was discovered. After Tsvang et al. (1991) failed to specifically highlight it, Foken (1990) and Panin et al. (1998) looked into it. However, a field study conducted in Tartu, Estonia, in 1990 (Foken et al. 1993), followed by an analysis in Kursk, Russia, in 1991, had as their goal to look into the surface.

Over the past ten years, this method has become considerably more accurate due to advancements in sensors, correction techniques, and the application of stricter data quality assessment (Foken et al. 2004; Moncrieff 2004; Mauder and Foken 2006; Mauder et al. 2007). Additionally, the eddy covariance observations' data quality examination (Mauder et al. 2006) had no appreciable impact. Even with the careful application of all turbulent flux adjustments, the residue can only be marginally reduced *(Foken et al. 2010; Mauder and Foken 2006, 2008).*

In 1989, Kansas, USA, hosted the first International Satellite Land Surface Climatology Project (ISLSCP) Field Experiment (FIFE). Although other FIFE experiments that were published said that the energy balance was closed, G. N. Panin also discovered an unclosed energy balance there *(Kanemasu et al. 1992).* Blanford et al. (1991) and Bernhofer (1992a), who was the first to apply large-scale non-turbulent transport processes to explain the flow underestimate, both produced groundbreaking work on the SEB closure problem. Ten years later *(Aubinet et al. 2000; Wilson et al. 2002),* ecological networks were utilized to solve the problem, and a first adjustment for general flow measurements was proposed *(Twine et al. 2000).*

2.6. Mathematical foundation

The so-called Reynolds decomposition is required to divide each variable's time series into a time-mean component and a fluctuating part to describe turbulent motions accurately.

Given as:

$$\zeta = \bar{\zeta} + \zeta' \tag{2.1}$$

and $$\bar{\zeta} = \frac{1}{T}\int_{t}^{t+T} \zeta(t)dt \tag{2.2}$$

The description of turbulent motions in the following theory sections requires the decomposition of the time series of each variable ζ into a time-mean part, $\bar{\zeta}$, and a fluctuating part, ζ'.

The following Reynolds postulates result from the use of Reynolds decomposition, which calls for averaging guidelines for the turbulent value:

I. $\overline{\zeta'} = 0$

II. $\bar{\zeta}\bar{\xi} = \overline{\bar{\zeta}\bar{\xi}} + \overline{\zeta'\xi'}$

III. $\overline{\bar{\zeta}'\bar{\xi}} = \bar{\bar{\zeta}}\,\bar{\xi}$

IV. $\overline{a\zeta} = a\bar{\zeta}$

V. $\overline{\zeta + \xi} = \bar{\zeta} + \bar{\xi}$ (2.3)

where a is a fixed value, only when averages are computed using "ensemble" averaging, which in this study meant taking the average of 30 minutes' worth of realizations made under identical conditions, are these correlations accurate *(Finnigan and Kaimal, et al. 1994)*.

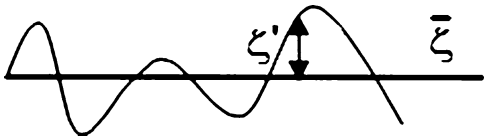

Figure 2.1. Schematic presentation of Reynolds decomposition of the value ς (Foken et.al. 2008).

The mass and the number of moles of an atmospheric ingredient, denoted as Ş, are represented by density (p_s, kg m^{-3}) and molar concentration (c_s, mol m^{-3}), respectively. The ideal gas and Dalton laws are related to these substances. Only the molar and mass mixing ratios are conserved quantities despite changes in temperature, pressure, and water vapor content (*Kowalski, Serrano-Ortiz et al(2007).*

The mass mixing ratio, which describes any scalar or vector quantity in the atmosphere, is used in the established one-point conservation equations. It is characterized by.

$$\frac{\partial \rho_d \zeta}{\partial t} + \vec{\nabla}\,(\vec{u}\rho_d\zeta) + K_\zeta \Delta(\rho_d\zeta) = S_\zeta \qquad (2.4)$$

where $\vec{u}$ is the wind velocity vector. $\vec{\nabla}$ and Δ represents the divergence $\left(\frac{\partial}{\partial_x}, \frac{\partial}{\partial_y}, \frac{\partial}{\partial_z}\right)$ and Laplacian $\left(\frac{\partial^2}{\partial_{x^2}}, \frac{\partial^2}{\partial_{y^2}}, \frac{\partial^2}{\partial_{z^2}}\right)$ operators, ρ_d is the dry air density. K_ζ is the molecular diffusivity of the quantity ζ, and S_ζ represent its source/sink strength. The equations describe Navier Stokes equations.

Application of these equations to the surface boundary layer requires the implementation of the Reynolds decomposition rules: the variables; p_d; u, and S_ζ should each be decomposed into a mean and a fluctuating part according to Equation 2.4, followed by application of the averaging operator, and appropriate rearrangement and simplification. By replacing ζ in equation 2.1 with equation 2.4, one obtains

$$\frac{\partial \rho_d}{\partial t} + \vec{\nabla}\,(\vec{u}\,\rho_d) = 0 \qquad (2.5)$$

Application of the time-averaging operator gives immediate:

$$\overline{\frac{\partial \rho_d}{\partial t}} + \vec{\nabla}\left(\overline{\vec{u}\rho_{dU_i}}\right) = 0 \qquad (2.6)$$

By replacing ζ in Equation 2.4 with the component of wind velocity in one given direction, u_i, one obtains the momentum conservation equation in this direction:

$$\frac{\partial \rho_{dU_i}}{\partial t} + \vec{\nabla}\left(\vec{u}\rho_{dU_i}\right) = 0 \qquad (2.7)$$

Forces serve as the momentum source/sink and are the source/sink terms in equation 2.7. On-air parcels in the atmospheric boundary layer may be subject to forces such as drag, pressure gradient, Coriolis, viscosity, and buoyancy. The first three forces are viewed as minor (i.e., not including vegetation) on a flat, horizontally uniform surface boundary layer above the roughness elements *(Foken et al. 2008; Stull et al. 2008).*

$$\frac{\partial \rho_{du}}{\partial t} + \frac{\partial \rho_{du^2}}{\partial x} +, \frac{\partial \rho_{dvu}}{\partial y} + \frac{\partial \rho_{dwu}}{\partial z} = 0 \qquad (2.8)$$

The Boussinesq-approximation (*Boussinesq et al. 1877*) ignores density fluctuations aside from in the buoyancy (gravitation) component due to the acceleration of gravity being particularly significant in comparison to the other accelerations in the momentum equation. Variables in italics can be eliminated by choosing a coordinate system in which v and w are zero, assuming horizontal homogeneity (which eliminates horizontal gradients), and steady-state conditions (which eliminate the time derivative).

$$\frac{\partial \overline{\acute{v}\acute{w}}}{\partial z} = 0 \qquad (2.9)$$

where $\overline{\acute{v}\acute{w}}$ is the eddy covariance term.

The scalar intensity of an atmospheric constituent was expressed in the conservation equation in terms of mixing ratio. The relation was determined from the settings in the data acquisition software, namely the maximum voltage output V_{max}, which relates to a maximum mixing ratio (density) of the trace gas x_{smax} (ρ_{smax}) and a zero voltage, which corresponds to a minimum mixing ratio (density) x_{smin} (ρ_{smin}):

$$x_s = x_{smin} + \frac{x_{smax} - x_{smin}}{v_{max}} V_x \quad (2.10)$$

$$\rho_s = \rho_{smin} + \frac{\rho_{smax} - \rho_{smin}}{V_{max}} V_p \quad (2.11)$$

x_{smax} (ρ_{smax}) as well as x_{smin} (ρ_{smin}) are there to maximize the analyzer's resolution and employ calibration gases with mixing ratios within this range, must be set by anticipated values of mixing ratios (densities) at the site. This formula for figuring out trace gas mixing ratios (densities) works with a lot of gas analyzers that provide analog output.

2.7. RStudio Software application

There were numerous software tools available in 2011 for processing eddy covariance data and calculating quantities like heat, momentum, and gas fluxes. The applications' complexity, adaptability, number of permitted instruments and variables, help system, and user assistance all differ greatly. While some software is closed-source or proprietary, some are open-source. Examples include commercial software, like the study's usage of EddyPro, which has a free license for non-commercial use. Free open-source software like ECO2S and ECpack and free closed-source software like EdiRe, TK3, Alteddy, and EddySoft are also used (*Mauder M. et al. 2007).*

CHAPTER THREE

3. Methodology

3.1. Data acquisition and data transfer

A sonic anemometer and an open-path infrared gas analyzer (IRGA) were deployed in Skukuza Kruger National Park as part of an eddy covariance system to measure energy flows on a yearly, seasonal, monthly, and daily basis and to measure Net Ecosystem Exchange (NEE). The IRGA monitors the air's carbon dioxide and water vapor concentrations, while the sonic anemometer measures wind speed and direction. To achieve reliable measurements, calibration of the gas analyzers and sonic anemometer was done frequently. To establish a correlation between the instrument response and real readings, calibration entails exposing the devices to known gas concentrations and wind speeds. Eddy covariance techniques are used on the raw data that has been obtained. These techniques establish the relationship between fluctuations in CO_2 and water vapor concentrations and the vertical wind speed. By using the raw observations in useful fluxes, this transformation reveals the patterns of energy exchange throughout the ecosystem.

The information we used was obtained over at least 18 years from the flux tower. A high frequency of at least 10 Hz was used to record the data to catch the rapid variations in atmospheric variables. The high-frequency data collected need to be averaged over 30 minutes. Averaging helps to reduce noise and enhances the signal of the fluxes being measured. The LI-7500 open-path analyzer, which measured CO_2 gas, instantaneous wind speed, CO_2 concentration, net radiation, and latent and sensible heat flux, was used to collect the data. It measured turbulent (vertical) fluxes of carbon dioxide, sensible heat, and latent heat for each 30-minute time step. Only in Skukuza, the area of interest, were fluctuations observed, therefore fetch/footprint was sufficient. Since the flow was only turbulent, Eddies were responsible for the majority of net vertical transfers.

3.2. Data post-processing and coverage

The eddy covariance techniques were used to process the data in order to obtain the fluxes of CO_2 and water vapor. Calculating the covariance between the variations in CO_2 and water vapor concentrations and vertical wind speed is required. The total energy balance and the net ecosystem exchange (NEE) at various time scales were obtained by integrating the fluxes over yearly, seasonal, monthly, and daily periods. Using the EddyPro software, a quality control phase is carried out to guarantee the dataset's dependability. This tool locates and eliminates outliers, systematic mistakes, and data gaps. Only data points with "good" (0) or "moderate" (1) quality flags are kept, guaranteeing that the analysis that follows is founded on factual and reliable data.

EddyPro software streamlines and automates the complex calculations and data processing required to interpret these fluctuations accurately. It assists in calculating fluxes of CO_2 and energy (sensible and latent heat) between the ecosystem and the atmosphere. The software uses algorithms to process the raw data collected from instruments such as sonic anemometers and gas analyzers, applying corrections for various factors such as air density changes, instrument calibration, and data filtering.

The tower data underwent quality assurance (if some data was outside the possible range, it was filtered out). Following *Foken et al. (2004).,* the quality flags were filtered using the EddyPro processing tool (only the good (0) and moderate (1) flags were used for further data analysis after obtaining the quality flag (QF) for each 30-minute data; flux data with quality flag 2(QF) was deleted. To guarantee that the dataset for the chosen water years was consistent and had more than 0% data available for analysis, data were further processed using the Reddyproc package in R statistical software. This technique was crucial to removing bias that might have been inherited from the data when comparing different years that weren't spread throughout seasons after bridging any gaps.

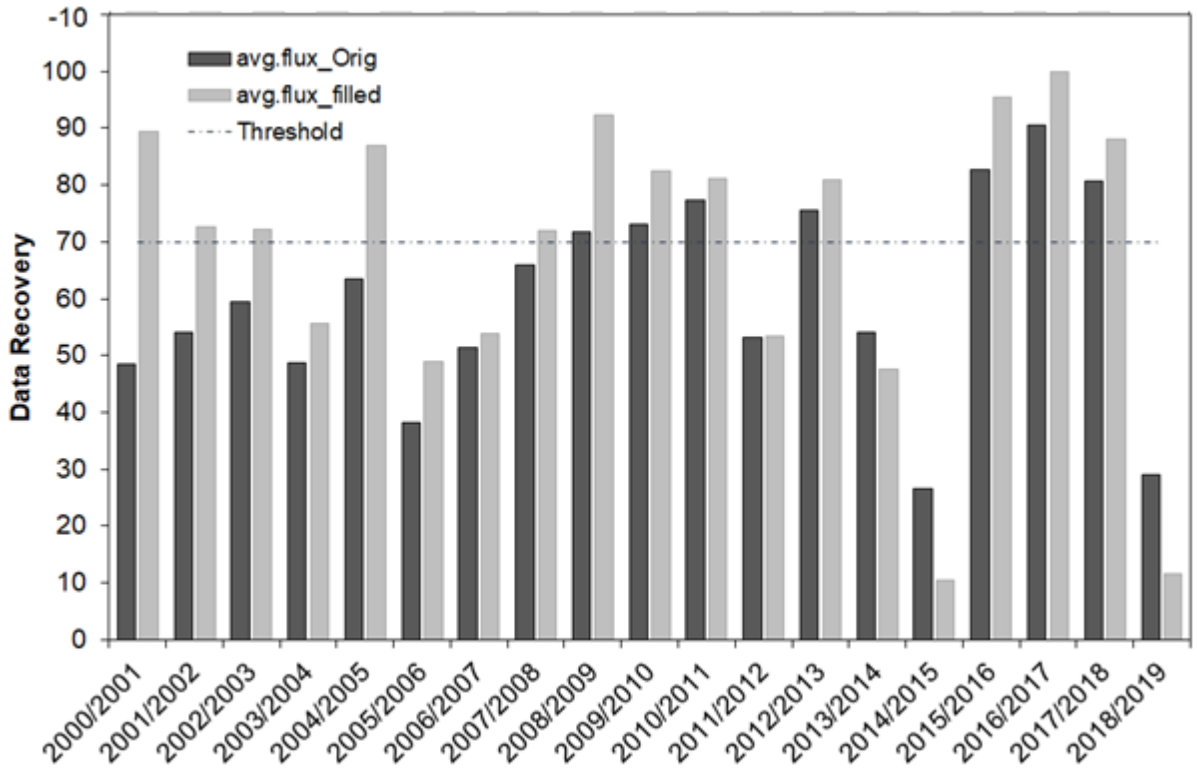

Figure 3.1. Mean annual rainfall and a dashed line are the mean rainfall from 2001 to 2018.

The study considered years with high rainfall to be above-average experienced by the site and years below rainfall to be low rainfall years. Figure 3.1 is the original measurements flux averaged across all five components (NEE, H, LE. Rn, G) and then averaged after a gap-filling with Reddyproc and filtered only to keep the most reliable data. Based on availability and to balance high and low rainfall years, a selection of four hydro-ecological years of the data collection, encompassing the years 2001/01/01 to 2018/12/31, was made. Another reason was that global temperatures have fluctuated according to worldwide metrological records, with some years recording higher temperatures than others. Over time, the temperature of the entire world increased, and South Africa was no exception. Among the hottest years on record were 2016 and 2017. Similar temperatures were experienced in 1998, 2005, 2009, 2010, 2012, and 2013. Due to this, both dry and rainy years were chosen for the study's sample period of 2008–2009, 2010–2011, 2015–2016, and 2017–2018.

3.3. CO_2 flux and energy flux determination

In this study, the Eddy flux *F* was calculated as follows :

$$F = \overline{\rho_a}\overline{W'S'} \quad (3.1)$$

The Eddy flux (F), which was about equal to the mean air density, was obtained by multiplying the mean air density by the mean covariance between variances in instantaneous vertical wind speed and mixing ratio. The equation represents the flux of a scalar quantity F, $\overline{\rho_a}$ the mean air density. $\overline{W'S'}$ is the time-averaged covariance between the turbulent fluctuations of vertical wind speed W' and the scalar S'. This term describes how turbulence transports the scalar quantity in the atmosphere.

The mean correlation between changes in instantaneous vertical wind speed and CO_2 air density was used to calculate the measured carbon dioxide flux or F_c *(Mauder M, Foken T, et al. (2011); Grünwald T, Bernhofer C et al 2011).*

$$F_C = \rho_a\overline{W'\rho_c'} \quad (3.2)$$

The covariance between the variances in instantaneous vertical wind speed and the temperature was used to calculate the sensible heat flux, *H*, which was then converted to energy units by adding the specific heat term is given in Equation 3.3:

$$H = \rho_a c_p \ \overline{W'T_a'} \quad (3.3)$$

Using water vapor, latent heat flux λE was calculated similarly and converted to energy units. This is represented by Equation 3.4:

$$\lambda E = \lambda\overline{W'\rho_v'} \quad (3.4)$$

In the above two equations, the meanings of the symbols are as follows: ρ_a denotes the density of dry air (kg m^{-3}) at a given air temperature, whereas c_p is the specific heat

capacity of dry air at constant pressure (J kg^{-1} K^{-1}), λ the latent heat of vaporization (J kg^{-1}), ρ_c the molar density of CO_2 gas (mol m^{-3}) and ρ_v the molar density of water vapour (mol m^{-3}). Furthermore, T_a represents the air temperature derived from the sonic anemometer (K) W the vertical wind velocity component (m s^{-1}), and the S' mixing ratios. Over bars denoted, time averages and primes indicated fluctuations in the averages.

3.4. CO_2 and energy flux corrections

The modification was necessary because changes in temperature and humidity can result in trace gas concentrations that are unrelated to the flux of the trace gas we are trying to detect. The WPL terminology for thermal expansion and water dilution are used by open-path instruments despite the fact that the long intake tubes muted high-speed temperature changes. These variables were modified to take into consideration the air's water vapor content and quick temperature changes, which had an impact on the calculated gas density*(Burba, G. et al. (2008)*.

$$F_{Ct} = F_{CO} + 1.6077 \frac{E_t}{\rho_d} \frac{q_c}{1+1.6077\frac{\rho_v}{\rho_d}} + \frac{S_s}{\rho C_P} \frac{q_c}{T_a} \quad (3.5)$$

where the various terms are explained as follows

F_{Ct}	Final flux
F_{CO}	Raw flux
$1.6077 \frac{E_t}{\rho_d} \frac{q_c}{1+1.6077\frac{\rho_v}{\rho_d}}$	Dilution Term
$\frac{S_s}{\rho C_P} \frac{q_c}{T_a}$	Expansion Term

To make up for the flux loss caused by the vertical wind speed and scalar sensors' inability to sample in the same volume, sensor separation was used. This was typically used for CO_2 fluxes, where "*T*" was frequently sampled by a sonic anemometer in the same volume as "*W*." *(Horst, et al.2003). This is implemented using Equation 3.6:*

$$T_s(n) = e^{-9.9(np_{xy}/\underline{U})^{1.5}} \quad (3.6)$$

where T_s symbolizes the transferred function for sensor separation, p_{yx} is the sensor separation distance, and U is the mean wind velocity. Furthermore, digital sampling was used to correct for aliasing. This was applied to all fluxes throughout the digital sampling, but it was frequently thought to be insignificant. *(Baldocchi, et al. 2005) The sampling* will *be represented by Equation 3.7:*

$$T_{ds} = 1 + (\frac{n}{n_s - n})^3 \quad (3.7)$$

where T_{ds} denoted the transferred function for digital sampling and n_s –the sampling frequency (for example 10 or 20 Hz). To make up for the flux that was lost due to the very small eddies that were lost when a path was averaged, volume and path averaging were accomplished. This was used for every scalar flow. The following is an equation for path averaging:

$$T_{SP}(n) = \sqrt{\frac{3+exp\left(-2\pi n\frac{p_s}{u}\right)-\left(\frac{4}{2\pi n\frac{p_s}{u}}\right)(1-exp)\left(-2\pi n\frac{p_s}{u}\right)}{2\pi n\frac{p_s}{u}}} \quad (3.8)$$

where T_{sp} symbolizes the – transferred function for scalar path averaging, p_s – scalar path length, and U – mean wind velocity. High-pass filters restored flux that was lost due to averaging, linear de-trending, or non-linear filtering when these processes were applied to all fluxes. An example of a recursive high-pass filter is: *(Baldocchi, et al. 2005).*

$$T_{hi}(n) = \frac{2\pi n\tau_f}{\sqrt{\frac{1+\frac{(2\pi n\tau_f)2}{1}}{\left(1+\frac{1}{\tau_f n_c}\right)}}} \quad (3.9)$$

where T_{hi} *was*– transferred function for high pass filtering, τ_f – high pass filter constant and n_c – cut-off frequency; ½ sampling frequency.

Webb Pearman Luening's term is applied to CO_2, *LE*, CH_4, or any other trace gas flux. The requisite equation was for open path Li 7500 (*Liu et al.2005). This is given in Equation 3.10 below:*

$$F_c = F_{c0} + \mu \frac{E}{\rho_d} \frac{q_c}{\mu + \frac{\rho_v}{\rho_d}} + \frac{H + q_c}{\rho C_p T_a} \tag{3.10}$$

where the symbols represent parameters as follows:

Table 3.1: Symbols and the Meanings of Parameters

F_c – final corrected flux	*q_c–meanCO_2 density*	*C_p – air, specific heat*
F_{co}– uncorrected flux	*ρ_d – dry air density*	*T_a– air temperature in K.*
E – evapotranspiration	*ρ_v– H_2O vapor density*	*μ –ratio of mol. masses of*
H– sensible heat flux	*ρ – total air density*	*air to water,* μ=*1.6077*

The loss of flux in the high-frequency portion of the co-spectrum, which was mostly brought on by the usage of anti-aliasing, was made up for by the low-pass filter. All fluxes were subjected to a filter. The following equation illustrates a post-field recursive low-pass filter (Baldocchi et al., 2001):

$$T_{lo}(n) = 1 - \frac{2\pi n \tau_f}{\sqrt{\frac{1 + \frac{(2\pi n \tau_f)^2}{1}}{\left(1 + \frac{1}{\tau_f n_c}\right)}}} \tag{3.11}$$

where $T_{lo}$is – transferred function for low-pass filtering, τ_f – low-pass filter constant, and n_c – cut-off frequency; ½ sampling frequency.

3.5. Data Analyses

A data analysis using R/RStudio was done to analyze the data to identify the drivers of the energy fluxes and the sources of variability. This involves correlating the fluxes with meteorological variables, land surface characteristics, and vegetation dynamics by ordinary least squares (OLS). Using OLS to examine the relationship between various environmental conditions and NEE (Net Ecosystem Exchange) and plotting diurnal, seasonal, and interannual fluctuations in NEE. Plotting hourly and daily values of NEE versus net radiation (Rn), heat flux (H), latent flux (LE), and soil heat(G), as well as sub-setting the data into daytime and nighttime values, are some of the specific techniques employed in the R script. The script also generates several graphs for additional investigation. R examines the variables influencing NEE in a savanna environment overall. The linear regression model is created using OLS regression method for analysis during water year, seasonal, and daily.

OLS regression is a commonly used method in statistics for modelling the relationship between a dependent variable in this case NEE and one or more independent variables of energy fluxes. The basic idea behind OLS is to fit a linear equation to the data that best explains the relationship. The assumptions about OLS are:

(a) Linearity: The relationship between the dependent and independent variable(s) is linear. This means that the change in the dependent variable for a unit change in the independent variable is constant.

(b) Independence: The observations are independent of each other. This means that the value of the dependent variable for one observation does not affect the value of the dependent variable for another observation.

(c) Homoscedasticity: The variance of the errors is constant across all values of the independent variable. This means that the spread of the errors is the same across all values of the independent variable.

(d) Normality: The errors are normally distributed. This means that the distribution of the errors follows a normal distribution.

(e) No multicollinearity: There is no perfect linear relationship between the independent variables. This means that the independent variables are not highly correlated with each other.

Table 3.2. Statistical tests for normality distribution

Distribution	KS statistic	Ks-p-value	AD statistic	Ad-p value	CV statistic	CV-p-value
Cauchy	0.08	0.48	1.46	0.19	0.14	0.41
Logistic	0.05	0.95	0.17	1.00	0.03	0.98
Normal	0.05	0.98	0.16	1.00	0.03	0.99

Table 3.2. displays the three different statistical tests for normality on the normal, Cauchy, and logistic distributions. The test distribution is listed in the first column, and the outcomes of the Kolmogorov-Smirnov (KS), Anderson-Darling (AD), and Cramér-von Mises (CV) tests are displayed in the subsequent columns.

A low p-value for the KS test signifies that the distribution under the test differs considerably from the normal distribution. Given that all three distributions in this situation have KS p-values over 0.48, there is no reason to doubt that they are all normal. Compared to the KS test, the AD test is more effective and offers a p-value. Again, the AD p-values for all three distributions are higher than 0.19, indicating that there is no reason to doubt that they are all normal. Similar to the KS test, the CV test is another test for normalcy. Once more, the CV p-values for all three distributions are higher than 0.41, indicating that there is insufficient data to disprove the null hypothesis that they are normal. The results in Table 3.2. for the normal distribution are similar to those for the logistic distribution, with small values for the goodness-of-fit statistics and high p-values, indicating a good fit.

CHAPTER FOUR

4. Results and discussions

4.1. Covariability between biometeorological and CO_2 flux exchange at semi-arid Skukuza Kruger National Park.

Data is gathered on biometeorological variables and CO_2 flux exchange over an extended period of time of 18 years in order to study the covariability between these variables. To do this, an eddy covariance tower and gas analyzers were used to find correlations, trends, and patterns between biometeorological variables and CO_2 flux exchange by examining the dataset in different time scales.

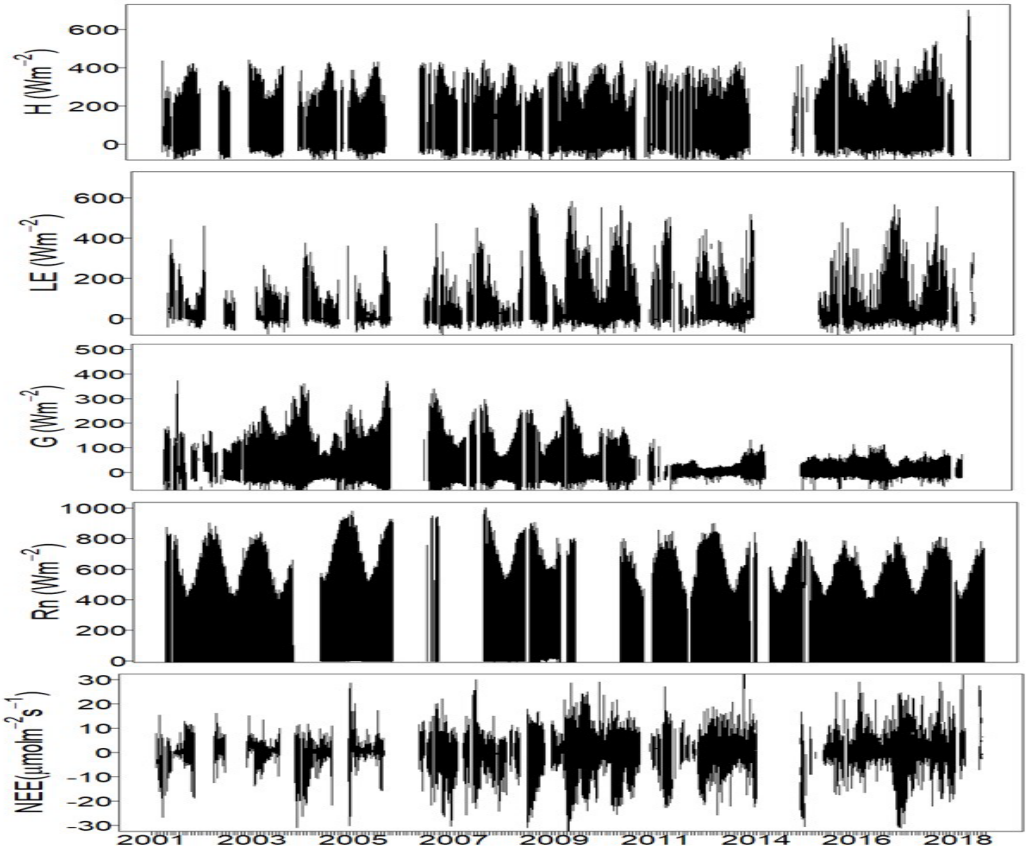

Figure 4.1. Gathered biometeorological sensible heat(H), latent heat(LE), ground(G), net radiation(Rn), and net ecosystem exchange(NEE or CO_2 flux) measurements.

Data was obtained from the Skukuza flux tower during 18 years, or from 2001 to 2018. The Skukuza ecosystem's biometeorological and flow dynamics are thoroughly understood thanks to this large dataset, which is also utilized to comprehend the fluxes in this area. The observations were used to assess how the effects of climate change will affect this ecosystem.

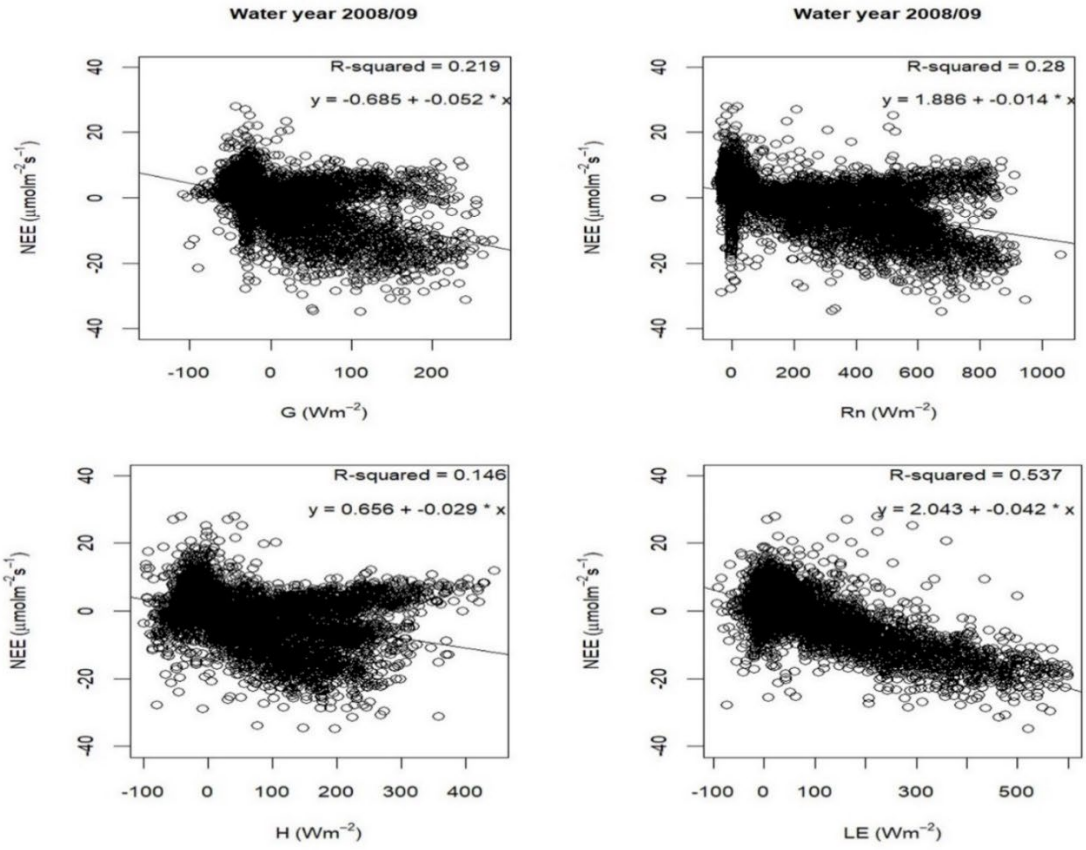

.

Figure 4.2. The correlation matrix pattern between CO_2 fluxes and energy fluxes of G, Rn, H, and LE using scatter plot for water year 2008-2009.

In the figure 4.2. , the water year 2008-2009, the relationship between NEE and G had a negative slope (y = -0.685+-0.052x) with a moderate r-squared value of 0.219. This suggests that an increase in G was associated with a decrease in NEE during this period. The relationship between NEE and Rn had a positive slope (y = 1.886+0.014x) with a slightly higher r-squared value of 0.28, indicating that an increase in Rn was associated with an increase in NEE.

The relationship between NEE and H had a relatively weak r-squared value of 0.146 with a positive slope [y = 0.656+-0.029x], indicating that an increase in H was associated with a slight increase in NEE. NEE and LE had a strong positive slope [y = 2.043+-0.042x] with a high *r*-squared value of 0.537, indicating that an increase in LE was associated with a significant increase in NEE.

Comparing the different relationships, it can be observed that the relationship between NEE and LE had the strongest association, followed by NEE and Rn. The relationships between NEE and G, and NEE and H, had weaker associations with NEE. The negative slope of the relationship between NEE and G suggests that the increase in G, which represents ground heat flux, may have led to a decrease in NEE, indicating that more carbon was being released into the atmosphere. The positive slope of the relationship between NEE and Rn suggests that more energy from the sun may have led to an increase in NEE, indicating that more carbon was being taken up by vegetation. The relatively weak relationship between NEE and H may suggest that changes in sensible heat flux have a weaker influence on NEE. Overall, the fluxes of energy and water have different impacts on NEE, and LE is likely a more important driver of NEE than G or H.

In the comparison of relationships, NEE's association with LE showed the strongest correlation, followed by NEE's correlation with Rn. NEE's associations with G and H were weaker. A decrease in NEE was indicated by the negative slope of NEE's relation with G, possibly due to heightened carbon release with increased ground heat flux. Conversely, the positive slope of NEE's relation with Rn suggested more carbon uptake with elevated solar energy. The relatively weak NEE-H relationship implied less influence of sensible heat flux changes. Overall, energy and water fluxes exerted distinct impacts on NEE, with LE likely exerting a more significant influence than G or H.

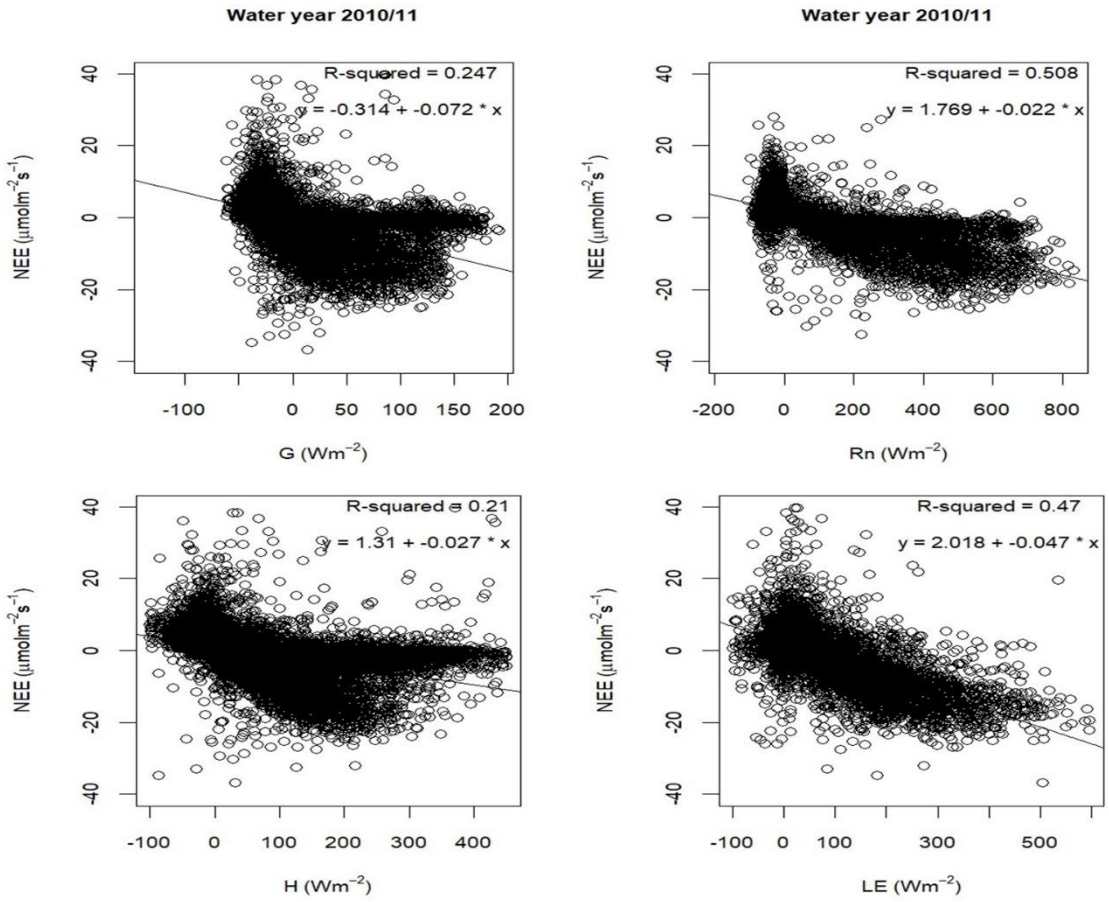

Figure 4.3. The linear correlation matrix pattern between CO_2 fluxes and energy fluxes using scatter plot for water year 2010-2011.

Figure 4.3. represents the slope of the linear regression models for NEE and G, Rn, H, and LE during the water year 2010-2011 are -0.314, 0.022, -0.027, and -0.047, respectively. The negative slope for NEE and G suggests that as G increases, NEE decreases, which indicates that the ecosystem is a carbon sink. The positive slope for NEE and Rn suggests that as Rn increases, NEE also increases, indicating that the ecosystem is a carbon source. The negative slope for NEE and H suggests that as H increases, NEE decreases, which indicates that the ecosystem is a carbon sink. The negative slope for NEE and LE suggests that as LE increases, NEE decreases, indicating that the ecosystem is a carbon sink. Comparing the slopes, we can see that the magnitude of the slopes for NEE and Rn and NEE and LE are greater than the magnitude of the slopes for NEE and G and NEE and H.

This suggests that Rn and LE have a stronger influence on NEE than G and H during the water year 2010-2011. However, it is important to note that the r-squared values for NEE and Rn and NEE and LE are also higher than the r-squared values for NEE and G and NEE and H, which indicates a better fit between NEE and Rn and LE compared to G and H. Rn and LE are more influential drivers of NEE than G and H during the water year 2010-2011. The key drivers of NEE during the water year 2010-2011 are Rn and LE, followed by G and H.

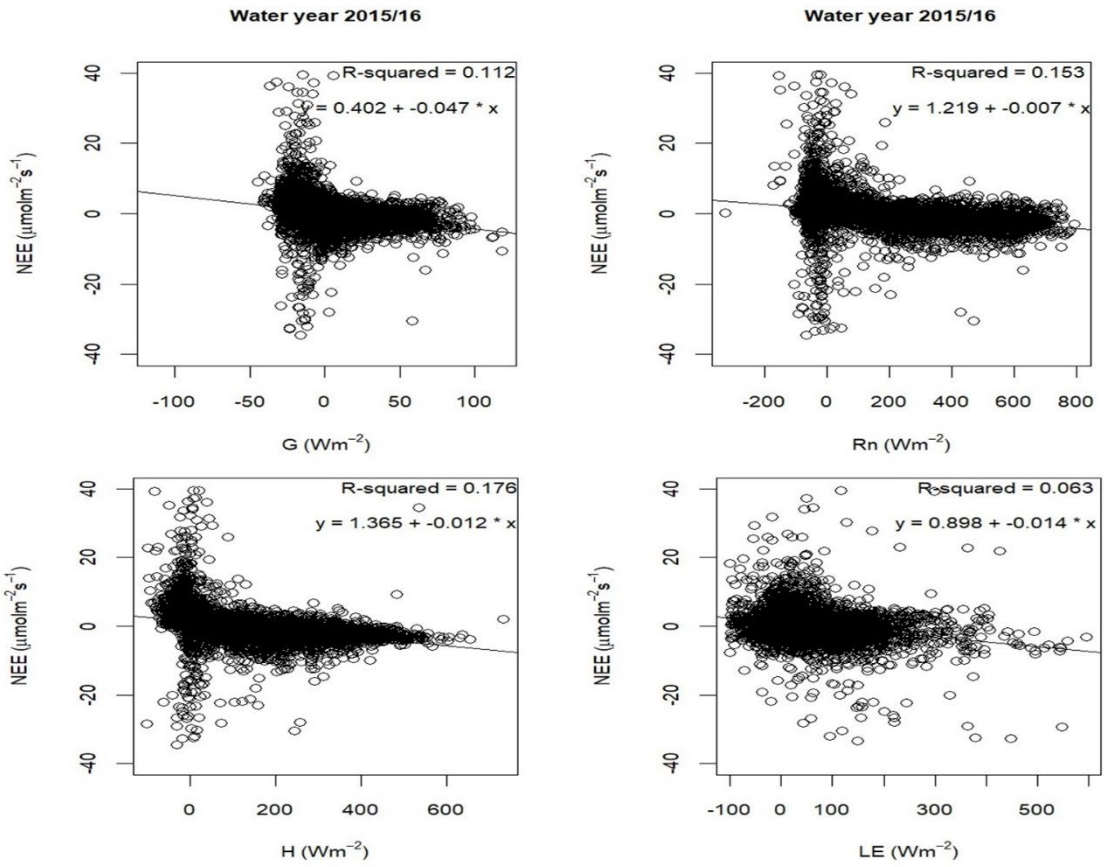

Figure 4.4. The correlation pattern between CO_2 fluxes and energy fluxes using a scatter plot for water year 2015-2016.

Figure 4.4. represents the water year 2015-2016, we can see that NEE is being compared with four different variables: G, Rn, H, and LE. The first comparison is NEE and G, which show a weak negative correlation with an r-squared value of 0.112 and a slope of -0.047. This indicates that there is a slight decrease in NEE as G increases.

The second comparison is NEE and Rn, which also shows a weak positive correlation with an r-squared value of 0.153 and a slope of 0.007. This suggests that there is a slight increase in NEE as Rn increases. The third comparison is NEE and H, which show a slightly stronger positive correlation with an r-squared value of 0.176 and a slope of -0.012. This suggests that there is a moderate increase in NEE as H increases. Finally, the fourth comparison is NEE and LE, which shows a weak positive correlation with an r-squared value of 0.063 and a slope of -0.014. This suggests that there is a slight increase in NEE as LE increases. NEE is influenced by multiple factors during the water year 2015-2016, with H being the most influential followed by Rn, G, and LE. However, it is important to note that the correlations between NEE and these variables are relatively weak. The drivers of NEE during the water year 2015-2016 are G (soil heat flux), Rn (net radiation), H (sensible heat flux), and LE (latent heat flux).

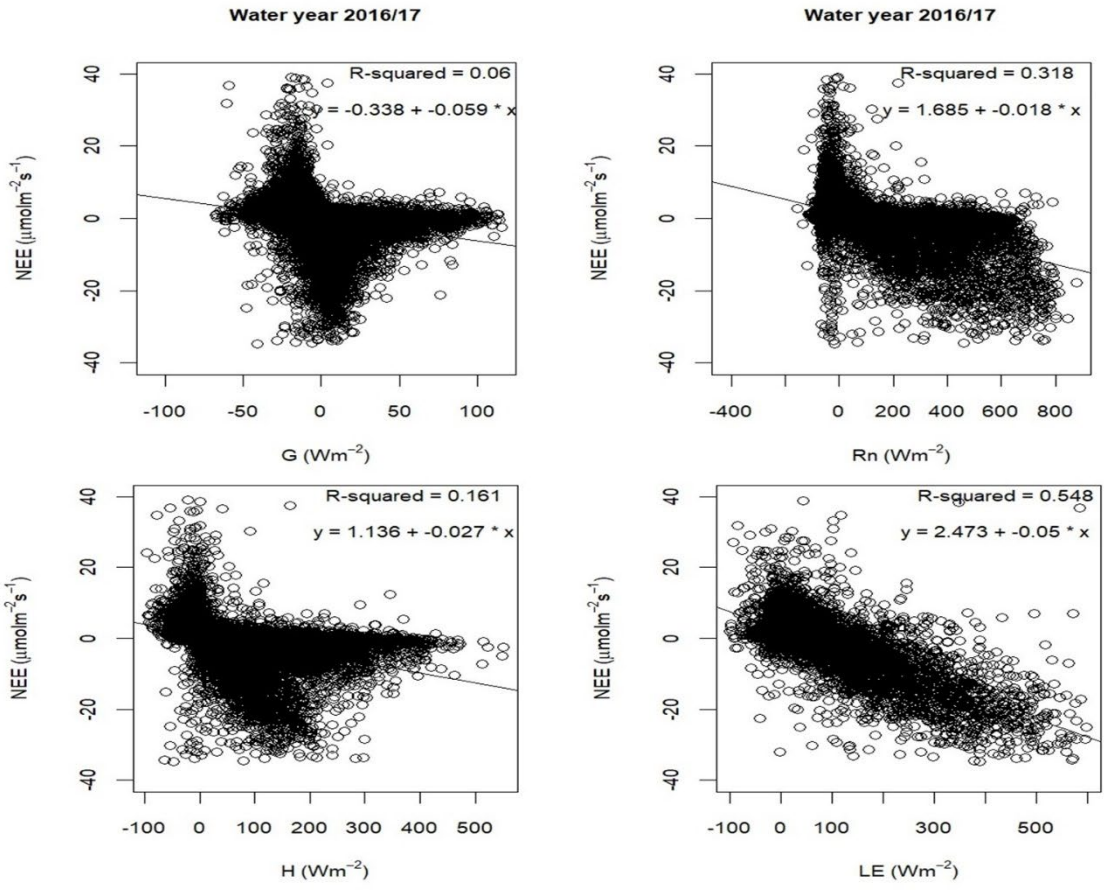

Figure 4.5. The correlation pattern between CO_2 fluxes and energy fluxes using a scatter plot for water year 2016-2017.

In Figure 4.5. the NEE data was analyzed with four different variables: G, Rn, H, and LE. The NEE and G relationship had a low r-squared value of 0.06, indicating a weak correlation between the two variables. The slope of the line is positive, indicating that an increase in G is associated with an increase in NEE. However, the small r-squared value suggests that G may not be a significant predictor of NEE this year. The NEE and Rn relationship had a slightly higher r-squared value of 0.318, indicating a moderate correlation between the two variables. The positive slope of the line also indicates that NEE tends to increase as Rn increases. However, the relatively low r-squared value suggests that Rn alone may not be a strong predictor of NEE this year.

The NEE and H relationship had a lower r-squared value of 0.161, indicating a weak correlation between the two variables. The negative slope of the line suggests that NEE tends to decrease as H increases. However, the small r-squared value suggests that H may not be a significant predictor of NEE in this year. Finally, the NEE and LE relationship had the highest r-squared value of 0.548, indicating a moderate to strong correlation between the two variables. The positive slope of the line suggests that NEE tends to increase as LE increases. The relatively high r-squared value suggests that LE may be a significant predictor of NEE in the year 2016-2017. NEE data in the water year 2016-2017 showed varying degrees of correlation with different environmental variables. LE was the variable with the highest correlation, followed by Rn, while H and G showed weaker correlations. The primary driver of NEE was latent heat flux (LE), followed by net radiation (Rn). This indicates that water availability and solar radiation played a significant role in regulating carbon uptake and release in the ecosystem. Sensible heat flux (H) and ground heat flux (G) showed weaker correlations with NEE, suggesting that they may have had a lesser impact on the carbon balance of the ecosystem during this year.

The NEE data showed variable associations with many environmental variables for the water year 2016–2017. Rn and LE showed the strongest connections, while H and G showed weaker relationships. The main cause of NEE was found to be latent heat flux (LE), with net radiation (Rn) having a significant supporting role.

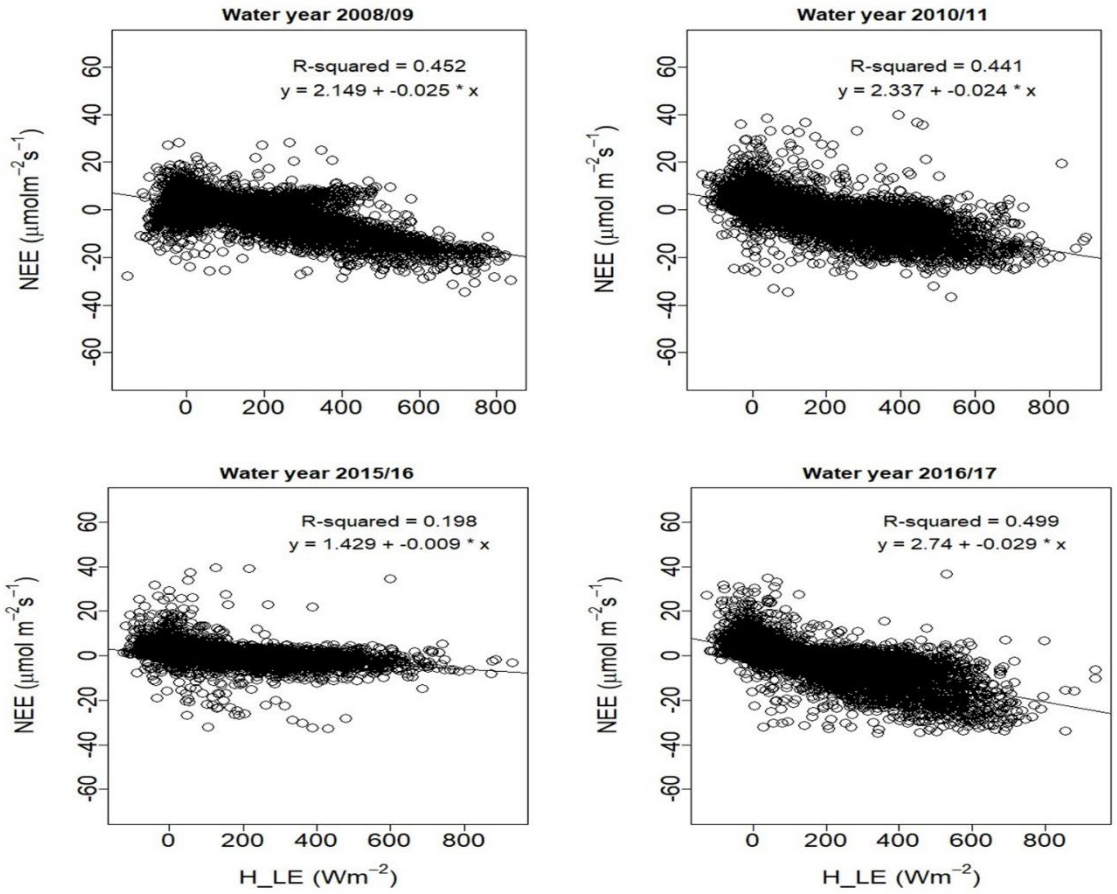

Figure 4.6. The correlation between NEE and H+LE energy fluxes using scatter plots during water years 2008-2009, 2010-2011, 2015-2016, and 2016-2017.

Figure 4.6. represents the NEE on the y-axis and H_LE on the x-axis indicating the relationship between net ecosystem exchange and latent heat flux. In the years 2008-2009 and 2010-2011, there is a moderate positive correlation between NEE and H_LE, as indicated by the r-squared values of 0.452 and 0.441, respectively. The slopes of these correlations are also positive, indicating that an increase in H_LE is associated with an increase in NEE. In the years 2015-2016, the correlation between NEE and H_LE is weaker, with an r-squared value of 0.198. The slope is still positive, indicating that an increase in H_LE is associated with an increase in NEE, but the relationship is not as strong as in the previous two water years. In the water year 2016-2017, there is a strong positive correlation between NEE and H_LE, as indicated by the r-squared value of 0.499. The slope is also positive, indicating that an increase in H_LE is associated with an

increase in NEE. There is a positive relationship between NEE and H_LE, meaning that as latent heat flux increases, net ecosystem exchange also tends to increase. This may indicate that higher rates of photosynthesis and carbon uptake are associated with higher rates of transpiration and water loss from the ecosystem. Drivers of NEE (net ecosystem exchange) are related to the H_LE (latent heat flux) energy fluxes.

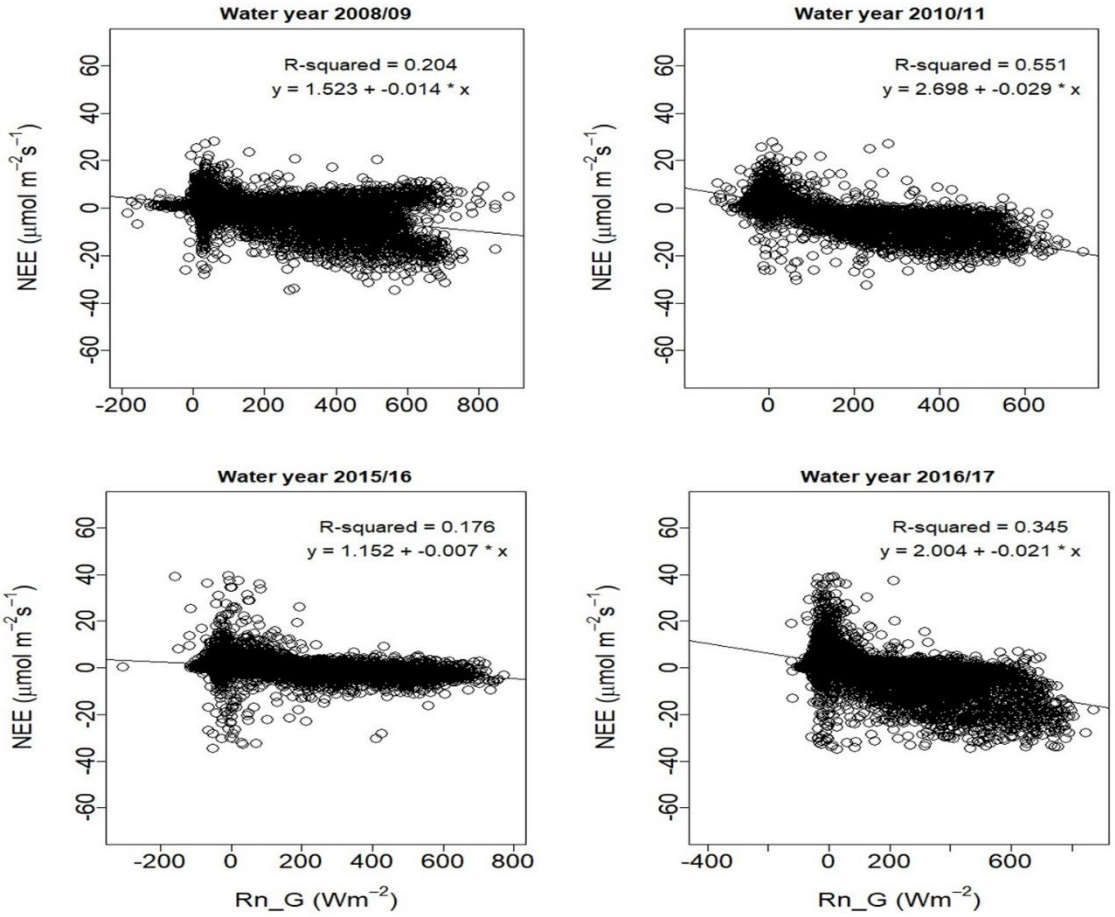

Figure 4.7. The correlation between NEE and Rn-G using scatter plots during water years 2008-2009, 2010-2011, 2015-2016, and 2016-2017.

In Figure 4.7., 2008-2009 and 2010-2011, there is a positive correlation between NEE and Rn-G, with moderate to strong r-squared values of 0.204 and 0.551, respectively. The slopes of the regression lines indicate that for every unit increase in Rn-G, NEE increases by 1.523 and 2.698, respectively. In 2015-2016, there is a weak positive correlation between NEE and Rn-G, with an r-squared value of 0.176. The slope of the regression line suggests that for every unit increase in Rn-G, NEE increases by 1.152,

which is smaller than the slopes observed in the previous two water years. In 2016-2017, there is a moderate positive correlation between NEE and Rn-G, with an r-squared value of 0.345. The slope of the regression line indicates that for every unit increase in Rn-G, NEE increases by 2.004, which is the highest slope observed among all the water years. The relationship between NEE and Rn-G can vary between water years, with some years showing stronger correlations than others. The slope of the regression line also varies between years, indicating that the effect of Rn-G on NEE can be stronger or weaker depending on the year.

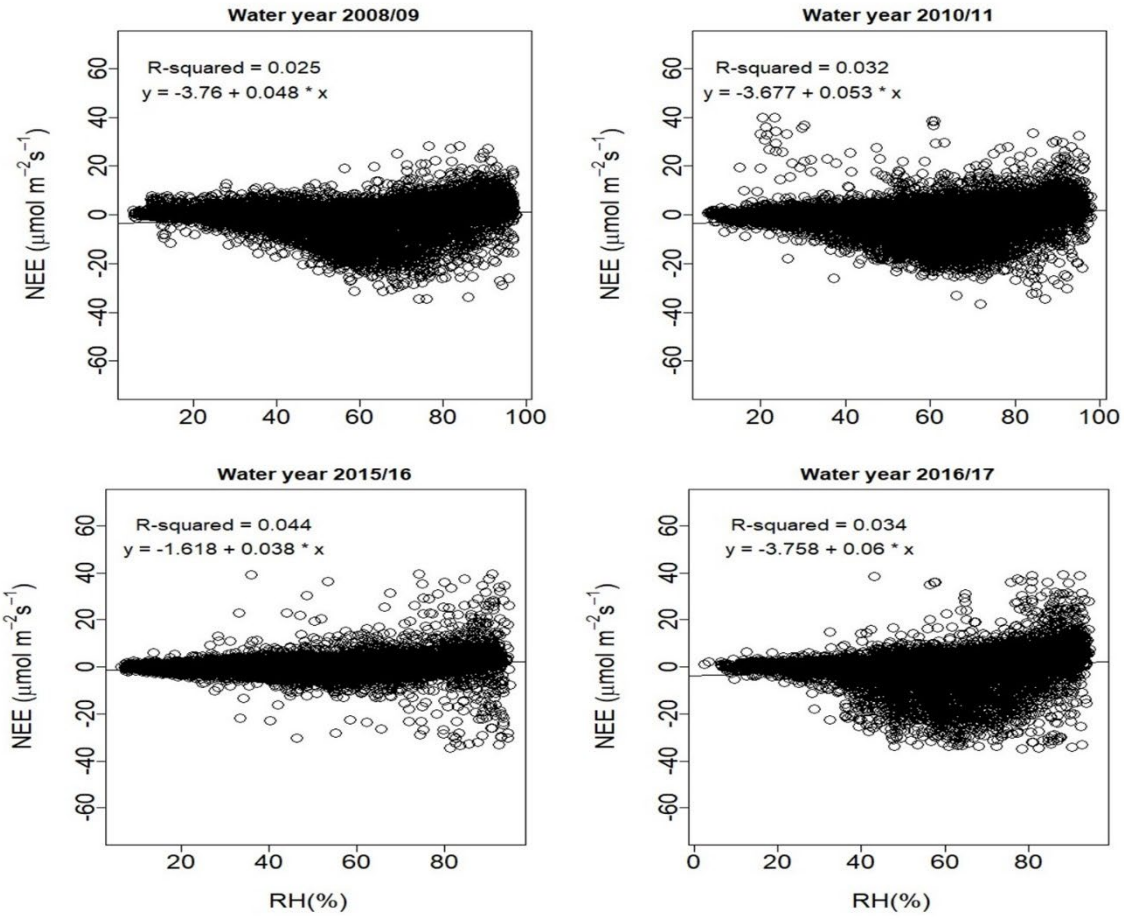

Figure 4.8. The correlation between NEE and RH using scatter plots for four water years 2008-2009, 2010-2011, 2015-2016, and 2016-2017.

Figure 4.8. represents two variables that have an extremely slender positive association. As a result, NEE and RH have a negligible yet favorable association with r^2 = 0.03 (2008/09), r^2 = 0.03 (2010/11), r^2 = 0.04 (2015/16), and r^2 = 0.03 (2016/17). Although there is little correlation, NEE tends to rise slightly when the relative humidity rises. The correlation value of 0.03 is quite near to 0, suggesting that there may be no real connection between NEE and RH.

Table 4.1. Summary of the results of NEE & intercept

	Coefficient	Std. error	t-value	p-value	95% CI Lower	95% CI Upper
Intercept	63.54	0.22	286.78	<0.001	63.11	63.98
NEE	0.52	0.03	15.56	<0.001	0.45	0.58

From Table 4.1. results of a statistical analysis involving the two variables "Intercept" and "NEE" are shown in the accompanying table. The dependent variable's estimated value when NEE is zero is indicated by the intercept value, which is 63.54. The dependent variable "NEE" is expected to increase by 0.52 units for every unit increase in NEE, as indicated by the coefficient of 0.52.

The r^2 numbers suggest a closer match as the standard errors represent the variability surrounding the regression line. High t-values (286.78 for the intercept and 15.56 for the NEE) highlight the weight of the evidence against the null hypothesis. The statistical significance of both coefficients is confirmed by P-values < 0.001. The 95% confidence intervals for the intercept and NEE provide a region where the true values are most likely to fall. These results suggest a positive relationship between NEE and the dependent variable, with both coefficients being highly significant and credible.

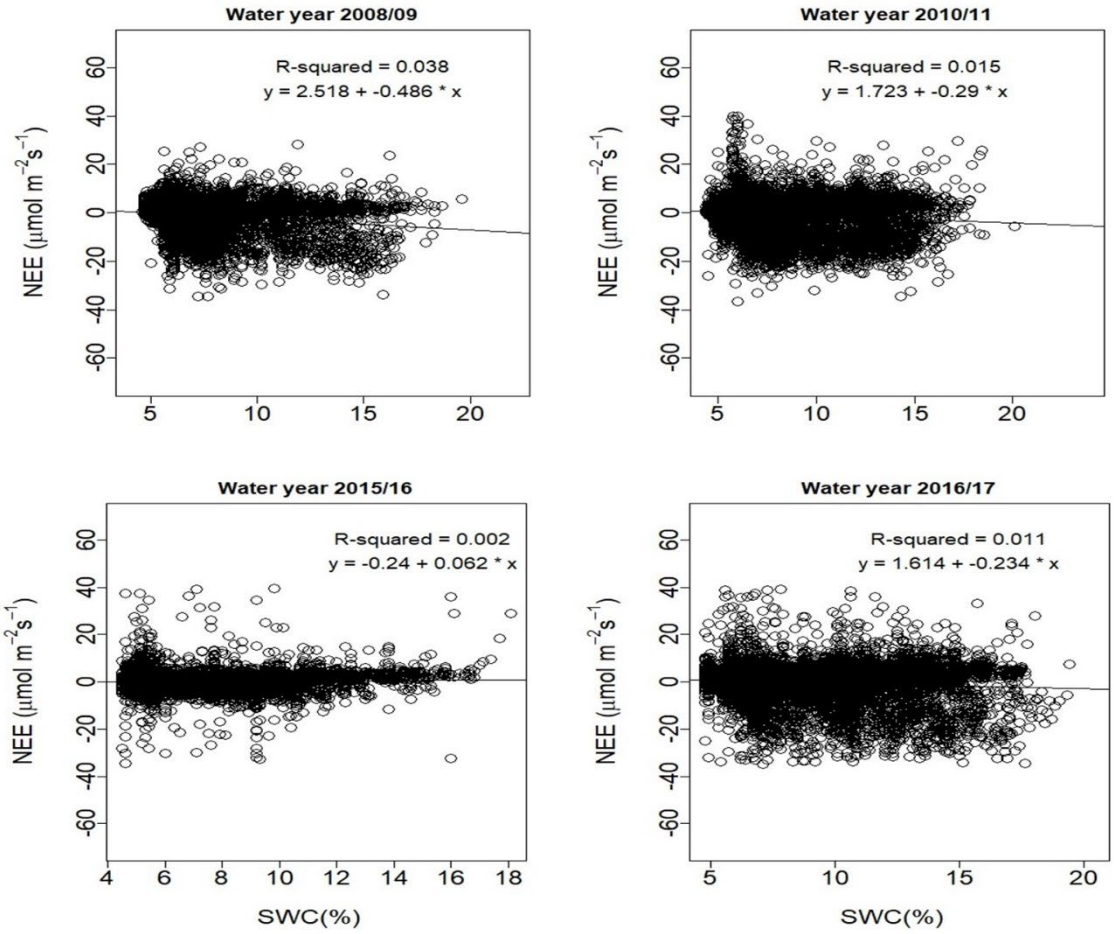

Figure 4.9. The correlation between NEE and SWC percentage using scatter plot during water year 2008-2009, 2010-2011, 2015-2016, and 2016-2017.

Figure 4.9. shows a weak correlation between NEE and SWC during the years 2008-2009 and 2010-2011, with low r-squared values and small slopes. This indicates that changes in SWC may not have a strong influence on NEE during these years. In contrast, during the water year 2015-2016, the correlation between NEE and SWC is very weak, with a very low r-squared value and a small positive slope. This suggests that there may not be a strong relationship between NEE and SWC during the 2015-2016 year. For the water year 2016-2017, there is a moderate correlation between NEE and SWC, with a larger slope and a higher r-squared value than the previous years. This suggests that changes in SWC may have a greater influence on NEE during this year. Overall, the relationship between NEE and SWC may vary depending on the water year and may not always be a strong predictor of NEE at Skukuza Kruger National Park.

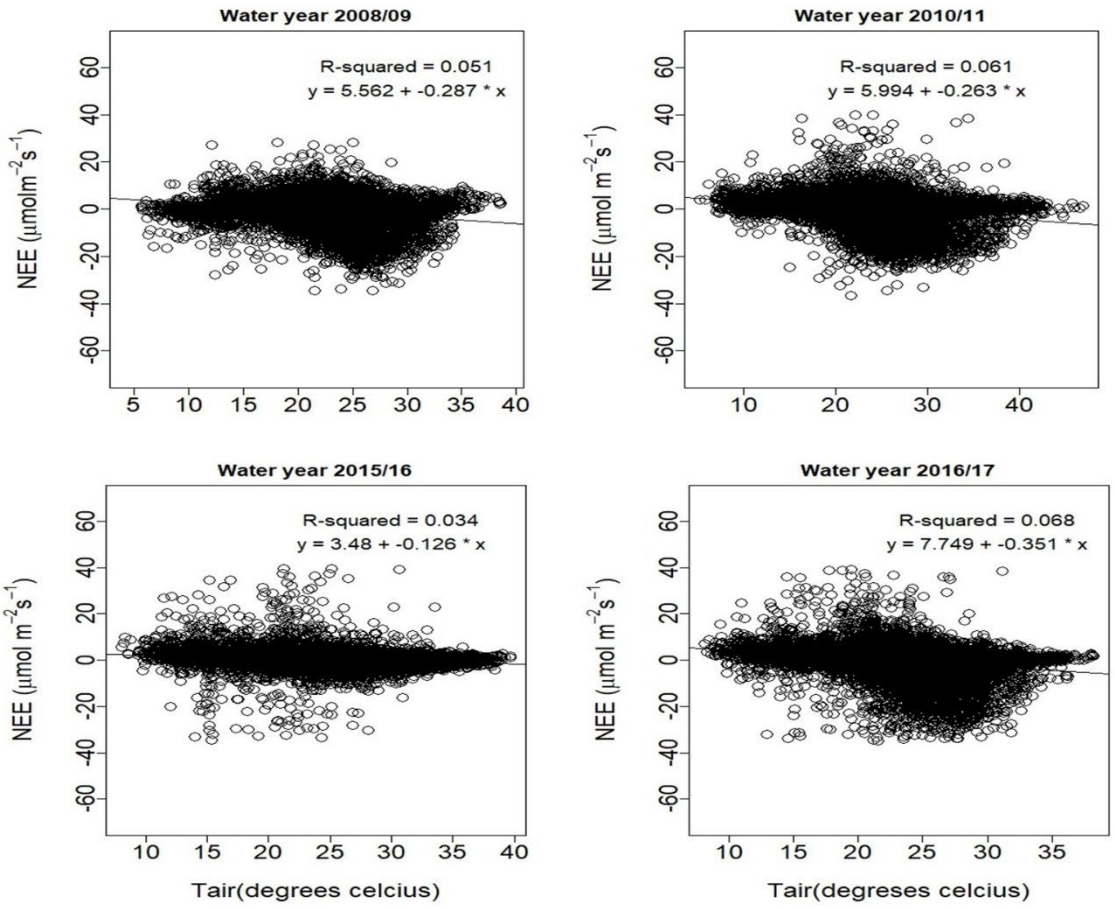

Figure 4.10. The correlation between NEE and Tair during water year 2008-2009, 2010-2011, 2015-2016, and 2016-2017.

Figure 4.10. indicates a weak correlation between NEE and T_{air} during the years 2008-2009 and 2010-2011, with r-squared values of 0.051 and 0.061, respectively. However, the slope is relatively high, indicating that a small increase in Tair results in a relatively large increase in NEE. Considering the water year of 2015-2016, the correlation between NEE and T_{air} is even weaker, with an r-squared value of 0.034, and a smaller equation of slope of y = 3.48+-0.126x. This may suggest that other environmental factors are dominating the relationship between NEE and T_{air} during this period. In the water year of 2016-2017, there is a moderate correlation between NEE and T_{air}, with an r-squared value of 0.068, and a relatively high slope of y = 7.749+-0.351x. This suggests that T_{air} is more dominant in influencing NEE during the 2016-2017 period compared to others.

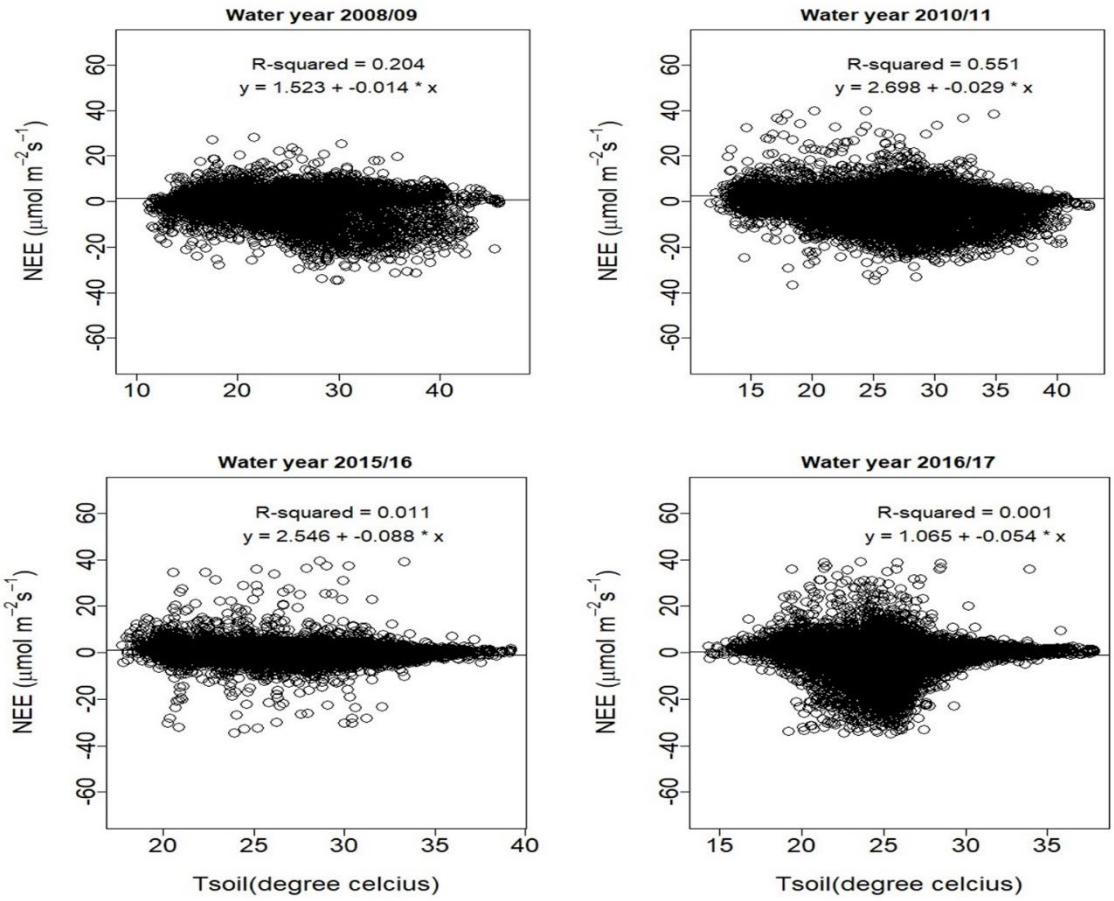

Figure 4.11. The correlation and regression model between NEE and T_{soil} during water year 2008-2009, 2010-2011, 2015-2016, and 2016-2017.

Figure 4.11. suggests a positive correlation between NEE and T_{soil} in the years 2008-2009 and 2010-2011, with a relatively stronger correlation observed in the latter year. However, in the years 2015-2016 and 2016-2017, the correlation appears to be weak, with r-squared values close to zero. The relationship between NEE and T_{soil} may vary depending on the water year, with stronger correlations observed in certain years and weaker or no correlations in others. Other factors, such as precipitation and vegetation dynamics, play a role in regulating the carbon balance.

Table 4.2. Statistical summary of measured NEE fluxes at various time intervals from the Gas analyzer.

Time Interval	Minimum NEE *(g C/m²)*	Maximum NEE *(g C/m²)*	Mean NEE *(g C/m²)*
30 minutes	-39.18784	39.92211	-0.0797489
Hourly	-35.39111	37.05662	-0.1620734
Daily	-7.436883	8.260898	-0.1014204
Monthly	-4.040636	1.530551	-0.130417

Table 4.2. represents NEE (Net Ecosystem Exchange) measurements for various time intervals: 30 minutes, hourly, daily, and monthly.

- **30 Minutes:** During 30-minute intervals, NEE values ranged between -39.18784 g C/m² (indicating carbon release) and 39.92211 g C/m² (indicating carbon uptake). On average, the ecosystem showed a slightly negative NEE value of -0.0797489 g C/m², suggesting a small net release of carbon over these short intervals.
- **Hourly:** In the hourly timeframe, NEE values varied from -35.39111 g C/m² to 37.05662 g C/m². The mean NEE value of -0.1620734 g C/m² indicates a slightly stronger trend of carbon release compared to the 30-minute intervals.
- **Daily:** On a daily basis, NEE fluctuated between -7.436883 g C/m² and 8.260898 g C/m². The mean NEE of -0.1014204 g C/m² suggests a modest net carbon release over the course of a day.
- **Monthly:** When considered on a monthly scale, NEE values ranged from -4.040636 g C/m² to 1.530551 g C/m². The mean NEE of -0.130417 g C/m² indicates a consistent pattern of carbon release over the span of a month.

These results depict the varying patterns of NEE across different time intervals, measured in grams of carbon per square meter (g C/m²). While there are fluctuations, the overall trend suggests that the ecosystem tends to release more carbon than it absorbs, with the extent of release differing based on the time interval considered. These insights contribute to our understanding of carbon dynamics and the ecosystem's response to changing conditions over different time scales.

4.2. Seasonal, monthly, and daily energy fluxes and NEE

Water availability and moderate temperatures during the rainy season often encourage plant growth and photosynthesis. While encouraging the breakdown and respiration of organic matter in the soil, the lower availability of water and elevated temperatures during the dry season might restrict plant development and photosynthesis.

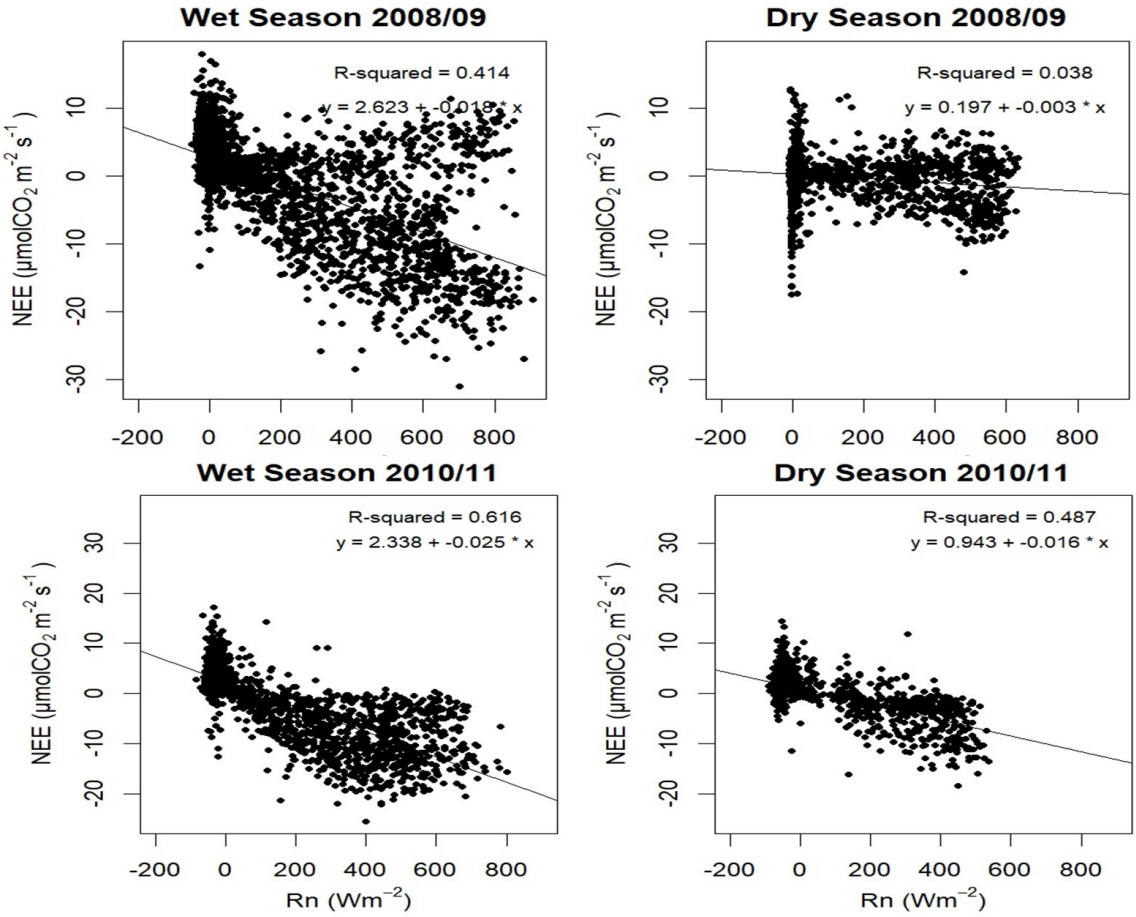

Figure 4.12. The correlation between net radiation and net ecosystem exchange during the wet and dry seasons of 2008-2009 and 2010-2011 water years.

Figure 4.12. shows that the correlation between NEE and Rn during the wet season of 2008-2009 is moderate (r-squared=0.414), and the slope of the line is positive, indicating that NEE increases with increasing Rn. This relationship is weaker during the dry season of 2008-2009 (r-squared=0.038), with a very low slope, suggesting that there is little or no relationship between NEE and Rn during this time. During the wet season of 2010-

2011, the correlation between NEE and Rn is stronger (r-squared=0.616), with a positive slope indicating that NEE increases with increasing Rn. This relationship is weaker during the dry season of 2010-2011 (r-squared=0.487), with a moderate slope, suggesting that there is still a positive relationship between NEE and Rn, but it is not as strong as during the wet season. Overall, there is a stronger positive relationship between NEE and Rn during the wet seasons compared to the dry seasons, which is expected given the role of moisture availability in controlling ecosystem processes. However, the strength of the relationship varies between wet seasons, with the wet season of 2010-2011 showing a stronger correlation than the wet season of 2008-2009.

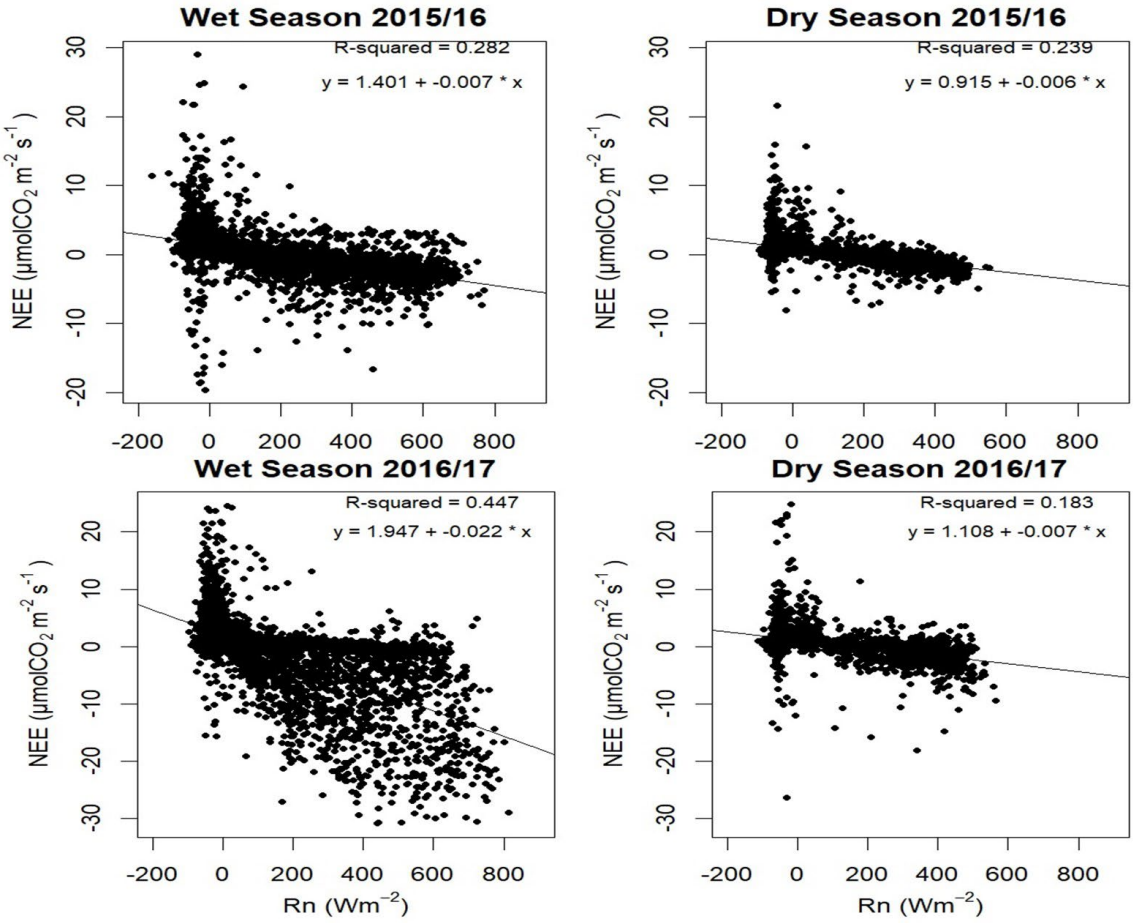

Figure 4.13. The correlation between net radiation and net ecosystem exchange during the wet and dry seasons of the 2015-2016 and 2016-2017 water years.

In Figure 4.13. the NEE and Rn have a positive association during the rainy seasons of 2015–2016 and 2016–2017. There is a proportional rise in NEE for every unit increase in Rn. The r-squared values for both wet seasons are, however, comparatively modest, suggesting that Rn may not be the only factor affecting NEE. In contrast, the association between NEE and Rn is weaker and has lower r-squared values during the dry seasons of both years. Additionally, the slopes of the regression equations are less, pointing to a weaker correlation between the variables. This shows that during the dry season, other environmental elements, such as soil moisture and temperature, may have a greater impact on NEE. The connection between Rn and NEE is strongest during the wet seasons and weaker during the dry seasons, and other factors may also play a role in influencing NEE.

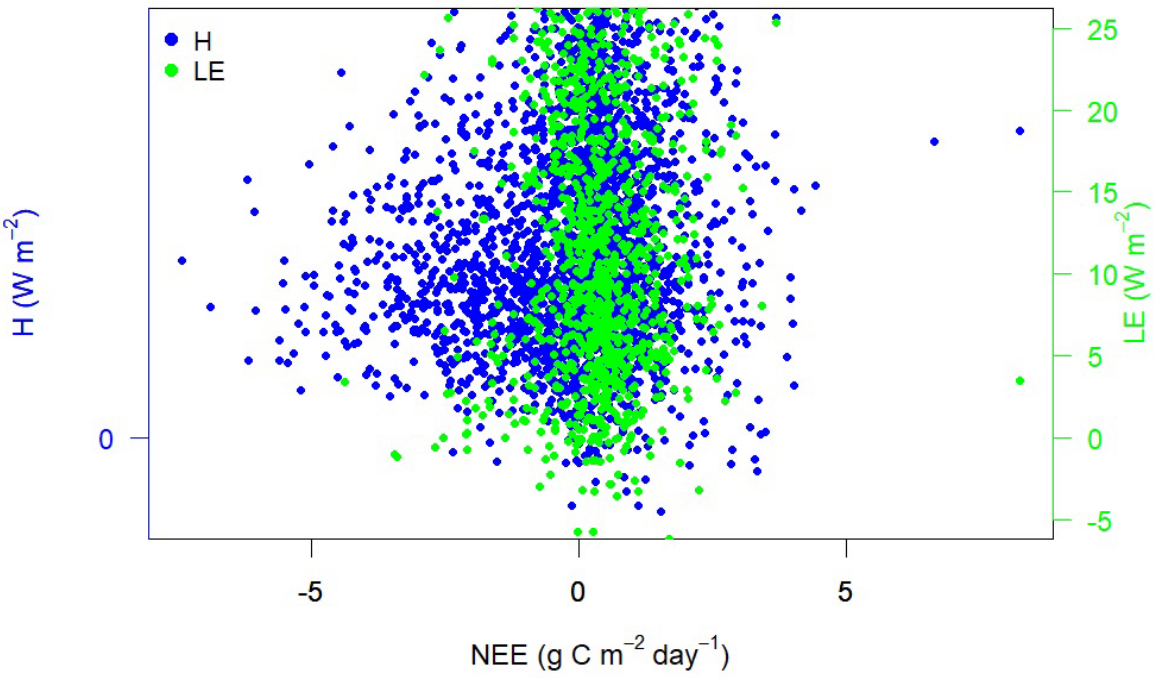

Figure 4.14. The NEE and energy fluxes of sensible heat and latent heat during the day.

The NEE ranges from -5 g C m^{-2} day^{-1} to +4 g C m^{-2} day^{-1}, and the energy of H and LE ranged between – 5 w/m^2 and + 25 w/m^2. In the given range of NEE (-5 g C m^{-2} day^{-1} to +4 g C m^{-2} day^{-1}), the ecosystem is sometimes a net carbon sink and sometimes a net carbon source, depending on the prevailing conditions. For instance, during the daytime, when photosynthesis is more active, the ecosystem may be a net carbon sink, leading to negative values of NEE. Conversely, during the nighttime, respiration dominates, leading to positive values of NEE as the ecosystem releases CO_2 into the atmosphere. According to the energy range for H (-5 w/m^2 to +25 w/m^2), depending on the direction of the flow, the sensible heat flux can have both cooling and heating effects. Similarly, the energy range for LE (-5 w/m^2 to +25 w/m^2) shows that depending on the flux's sign, the latent heat flux can have both water uptake and release effects.

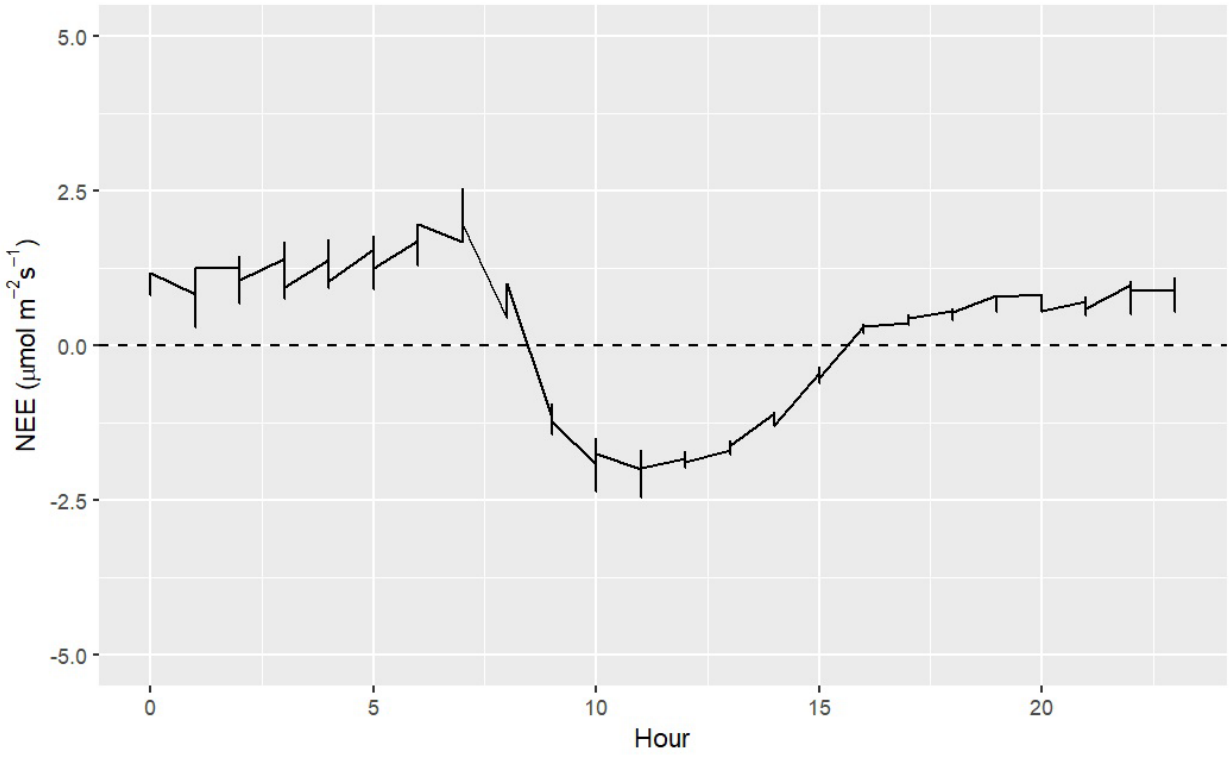

Figure 4.15. The Net Ecosystem Exchange (NEE) during the day. The Net Ecosystem Exchange (NEE) values are used to characterize the uptake and loss of CO_2 by an ecosystem for a day.

During the day, when sunlight is available, photosynthesis is more active, leading to a net uptake of CO_2 by the ecosystem. This uptake is reflected in the negative values of NEE, indicating that the ecosystem is a net carbon sink. However, during the night, photosynthesis stops, and respiration dominates, leading to a net release of CO_2 by the ecosystem. This release is reflected in the positive values of NEE, indicating that the ecosystem is a net carbon source.

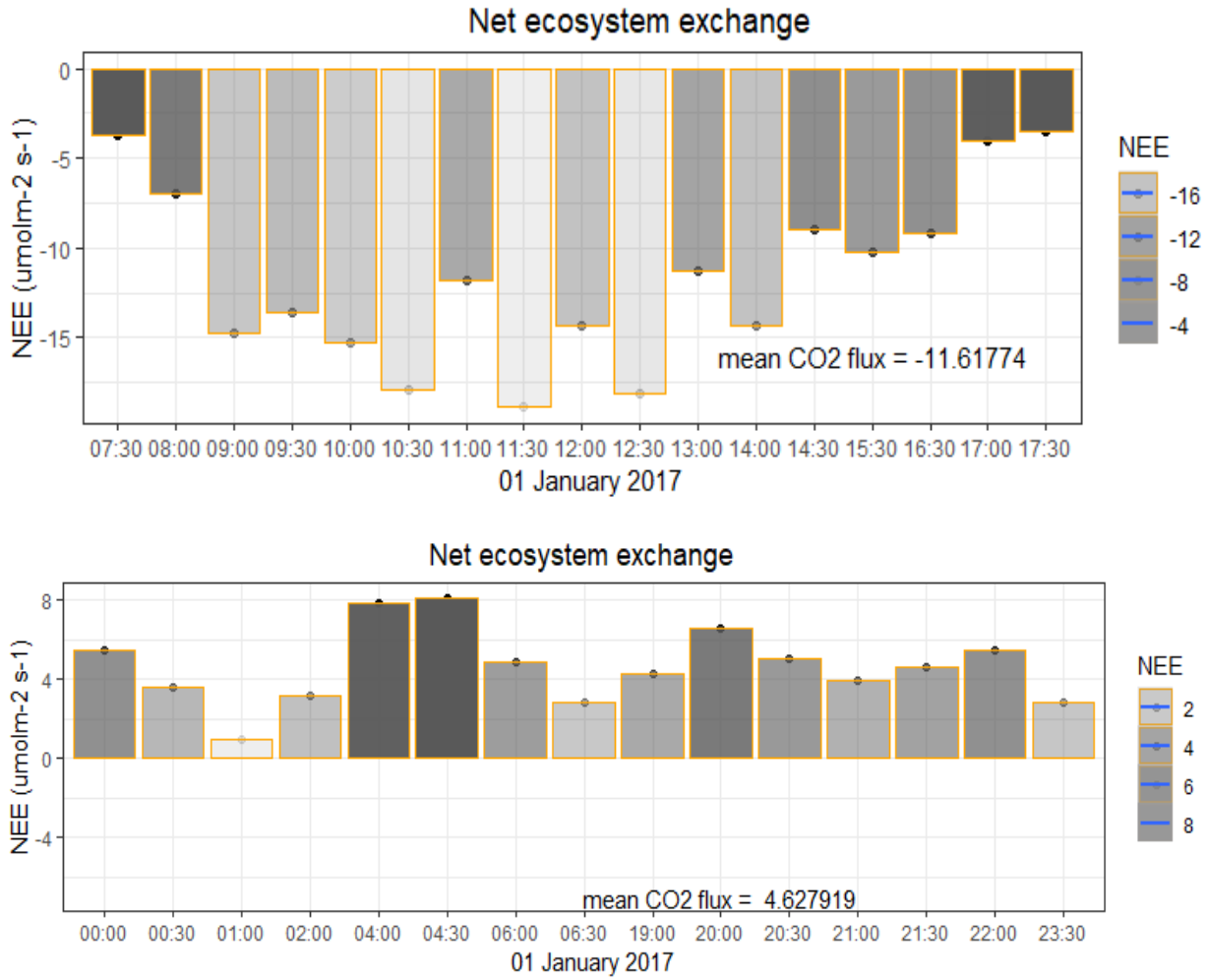

Figure 4.16. The Comparison of diurnal NEE for 01 January 2017.

Figure 4.16. represents average daytime NEE, which throughout this time was -11.6177 $\mu mol.m^{-2}.s^{-1}$, showing that the ecosystem functioned as a net carbon sink during the day. The ecosystem was a net carbon sink during the day, but at night, the average NEE was

+4.6354 μmol.m^{-2}.s^{-1}. This diurnal pattern of NEE is consistent with the idea that respiration predominates at night while photosynthesis predominates during the day.

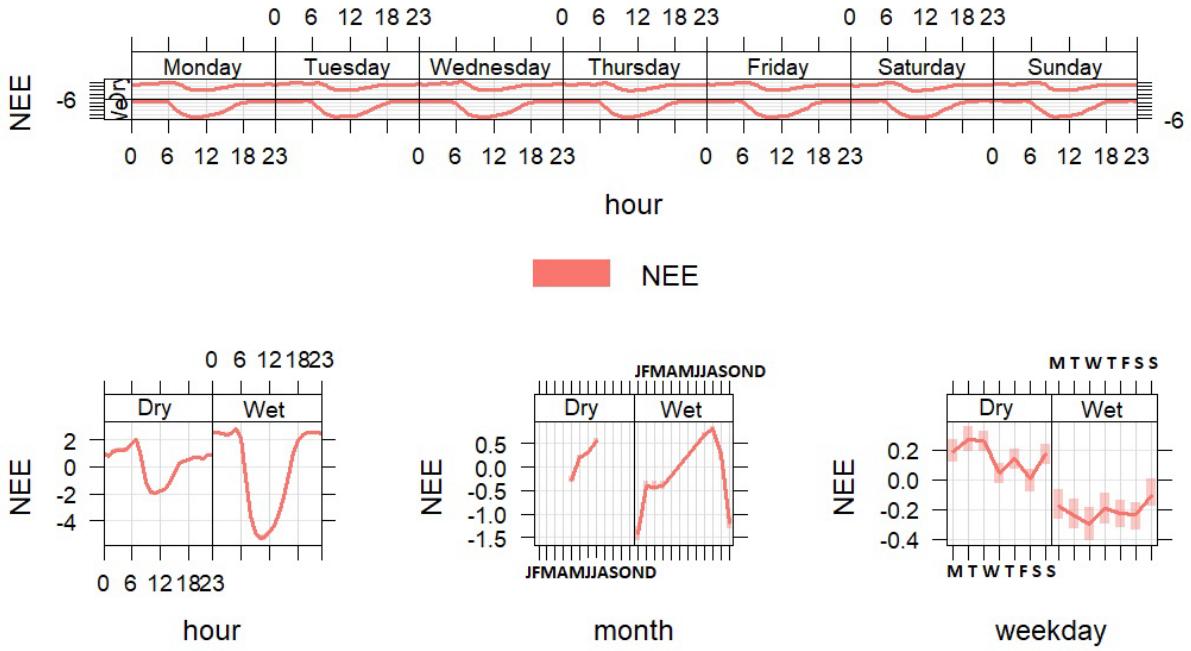

Figure 4.17. Overall view of NEE hourly, weekday, and monthly.

To understand the patterns in more detail, the analysis was done on a hydro-ecological year scale rather than an hourly, daily, weekday, or monthly scale, which allows for a more comprehensive assessment of the ecosystem's functioning over time. Overall, the data suggests that the ecosystem was becoming less efficient in sequestering carbon over time, likely due to changes in environmental conditions.

4.3. Energy closure

The energy closure principle can be viewed as a manifestation of the law of conservation of energy, which states that energy cannot be created or destroyed, only transformed from one form to another. The energy closure principle implies that the total amount of energy entering or leaving the system must be balanced, such that the sum of the energy fluxes measured or estimated at the surface of the ecosystem must equal the net radiation (Rn) received by the system. Energy closure refers to the degree to which the energy balance equation is satisfied within an ecosystem. The energy balance relation states that the sum of incoming and outgoing energy fluxes should be equal, i.e., the net radiation (Rn) equals the sum of sensible heat (H) and latent heat (LE) fluxes, as well as ground heat flux (G). This is given in Equation 4.1

$$Rn = H + LE + G \tag{4.1}$$

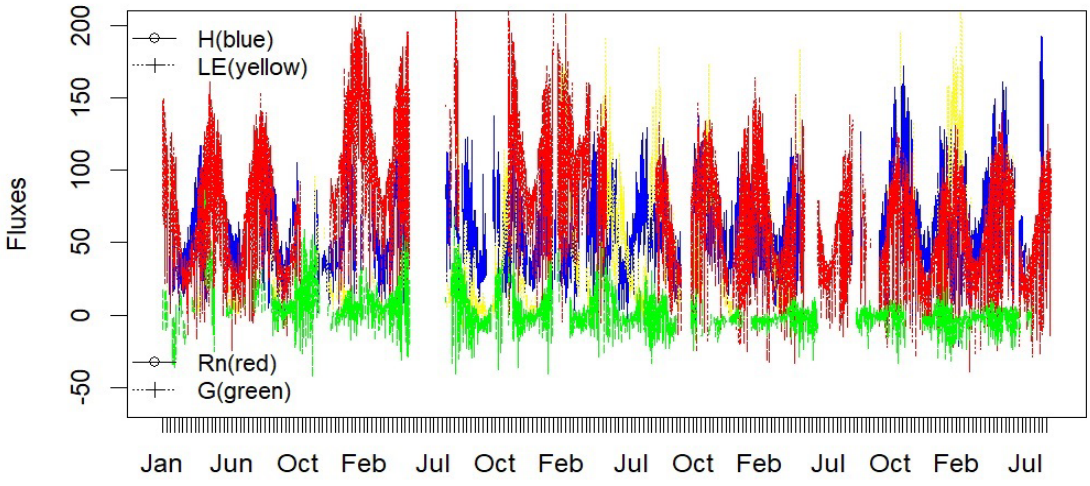

Figure 4.18. The energy fluxes of sensible heat(H-blue), latent heat(LE-yellow), ground heat(G-green), and incoming and outgoing radiation(Rn-red) from 2001-2018.

Figure 4.18. indicates the transmission of heat energy resulting from the temperature difference between the land surface and the air above it is known as the sensible heat flux (H). It is often positive during the day and negative at night. The exchange of water vapor between the ground surface and the atmosphere results in a heat energy transfer known as the latent heat flux (LE). It is typically positive during the day and at night, except when dew is forming. The movement of heat energy from the land surface to the subsurface soil layer is known as the ground heat flux (G). It has a smaller magnitude than the sensible and latent heat fluxes. The difference between the radiation that enters and leaves the land surface is known as the net radiation or Rn. It is often positive during the day and negative at night.

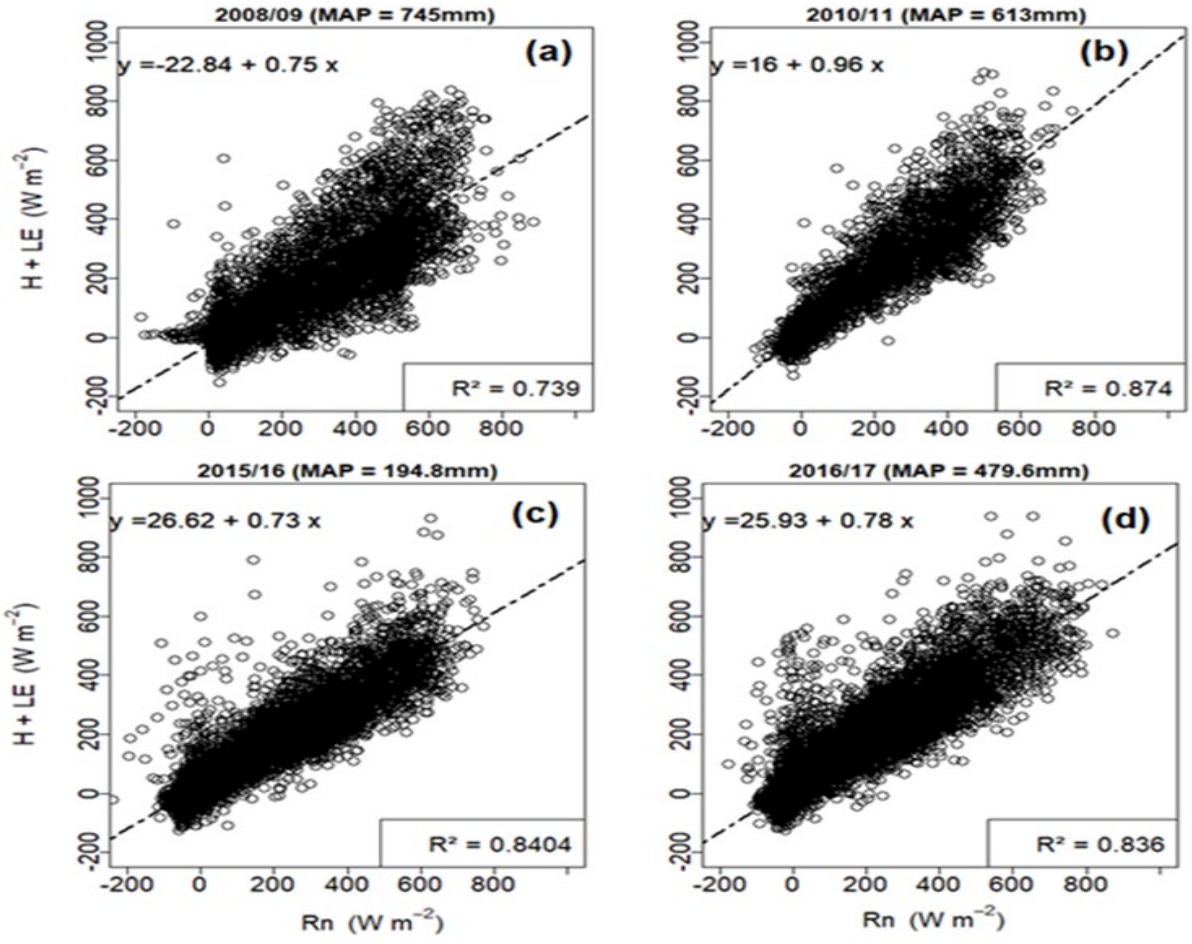

Figure 4.19. Energy closure for water year 2008-2009, 2010-2011, 2015-2016, 2016-2017.

The results are in Figure 4.19. show a positive correlation between H+LE+G and Rn, indicating that there is an increase in the sum of sensible heat flux, latent heat flux, and ground heat flux with an increase in net radiation. The strength of this correlation varies with the amount of annual precipitation, with higher correlation coefficients observed in wetter years. In the wetter years of 2008-2009 and 2010-2011, there is a strong positive correlation between H+LE+G and Rn, with r-squared values of 0.739 and 0.874, respectively. The regression lines for these years have slopes of 0.75 and 0.96, respectively, indicating a stronger relationship between H+LE+G and Rn in 2010-2011. In contrast, the correlation is weaker in the drier years of 2015-2016 and 2016-2017, with R-values of 0.84 and 0.836, respectively. The regression lines for these years have shallower slopes, indicating a weaker relationship between H+LE+G and Rn. Overall, these graphs suggest that the relationship between H+LE+G and Rn is influenced by the amount of annual precipitation, with a stronger relationship observed in wetter years.

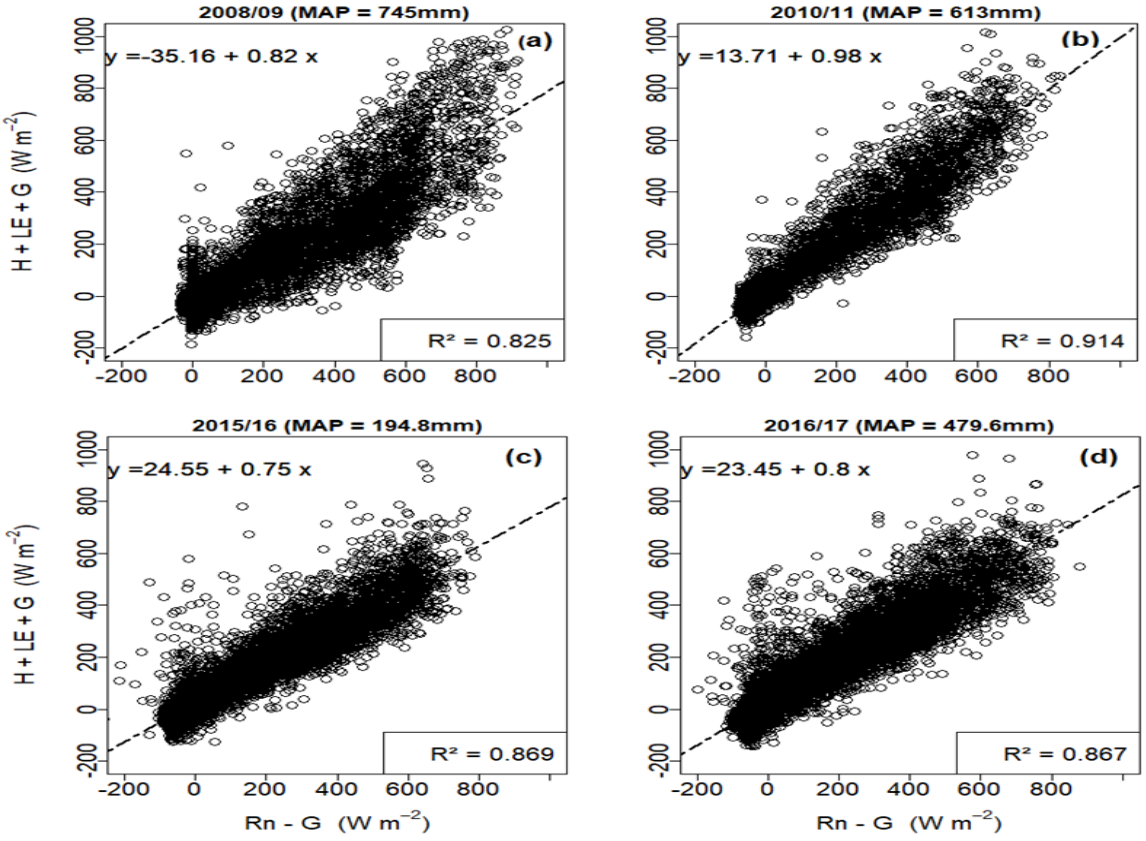

Figure 4.20. The surface energy closure for water years 2008-2009, 2010-2011, 2015-2016, and 2016-2017.

The graphs in Figure 4.20. shows the relationship between H+LE+G (sensible and latent heat fluxes) on the y-axis and Rn-G (net radiation minus soil heat flux) on the x-axis for four different years with varying mean annual precipitation (MAP). The regression lines show a positive correlation between H+LE+G and Rn-G in all four years. The strength of the correlation, as indicated by the r-squared values, ranges from 0.825 to 0.914, suggesting a strong linear relationship between the variables. Interestingly, the slope of the regression line varies between the years, with steeper slopes seen in the years with lower MAP values (2010-2011, 2015-2016, and 2016-2017). This suggests that the sensitivity of H+LE+G to Rn-G may increase during periods of lower precipitation. The results mean that there is a strong linear relationship between H+LE+G and Rn-G, and this relationship may be influenced by precipitation levels. These findings highlight the importance of considering precipitation variability when studying the surface energy balance and its components.

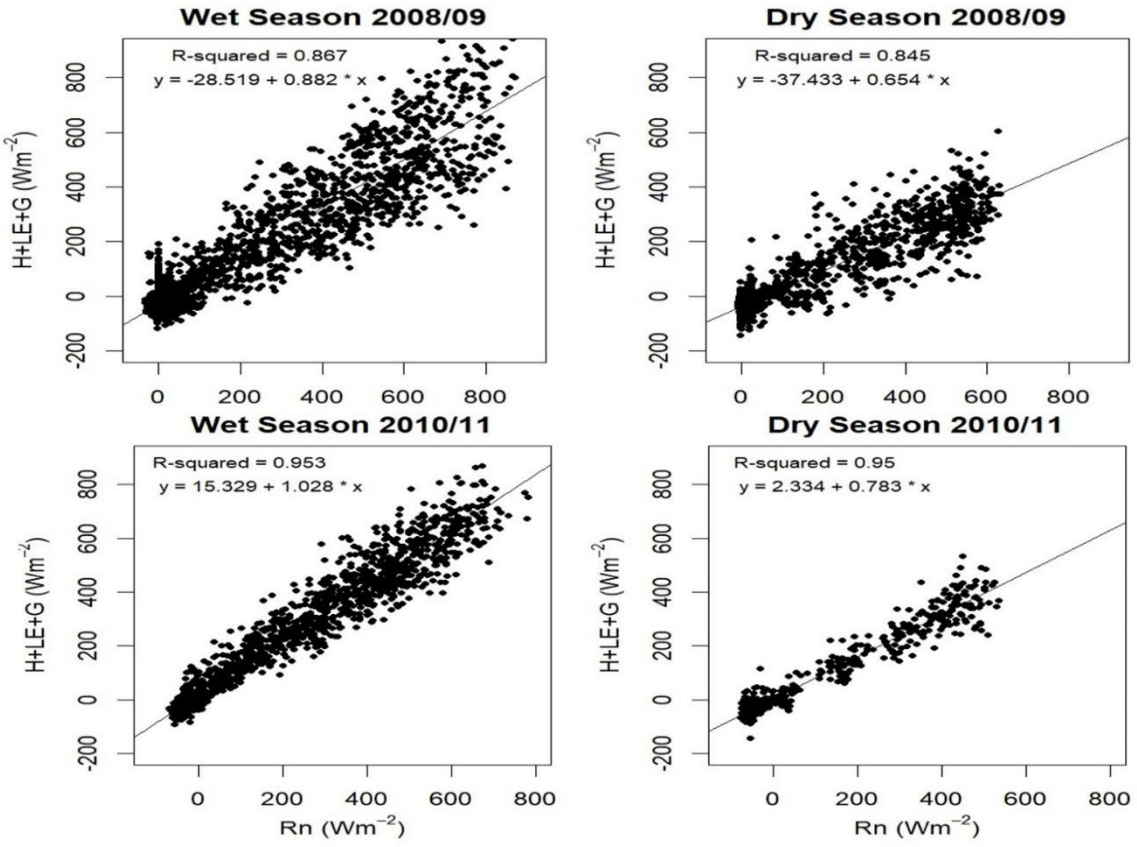

Figure 4.21. The energy closure for seasons 2008-2009, 2010-2011.

The graphs in Figure 4.21. suggest that there is a strong positive relationship between the H+LE+G and the Rn in all four seasons, as evidenced by the high values of the correlation coefficient R-squared. In the wet season of 2008-2009, there is a strong positive correlation (r=0.867) between the two variables, and the regression equation indicates that for each unit increase in Rn, H+LE+G increases by 0.882 units. The r-squared value of 0.867 suggests that 86.7% of the variation in H+LE+G can be explained by the variation in Rn in this season. In the dry season of 2008-2009, there is also a strong positive correlation (r=0.845) between the two variables, and the regression equation indicates that for each unit increase in Rn, H+LE+G increases by 0.654 units.

The r-squared value of 0.845 suggests that 84.5% of the variation in H+LE+G can be explained by the variation in Rn in this season. In the wet season of 2010-2011, there is an even stronger positive correlation (r=0.95) between the two variables, and the regression equation indicates that for each unit increase in Rn, H+LE+G increases by 1.028 units. The R-squared value of 0.95 suggests that 95% of the variation in H+LE+G can be explained by the variation in Rn in this season.

In the dry season of 2010-2011, there is also a strong positive correlation (r=0.95) between the two variables, and the regression equation indicates that for each unit increase in Rn, H+LE+G increases by 0.783 units. The R-squared value of 0.95 suggests that 95% of the variation in H+LE+G can be explained by the variation in Rn in this season. The results suggest that there is a strong positive relationship between the two variables in all four seasons, and the models provide a good fit for the data. The regression equations can be used to predict the value of H+LE+G for a given value of Rn in each season, and the high R-squared values indicate that the model explains a large proportion of the variation in the dependent variable.

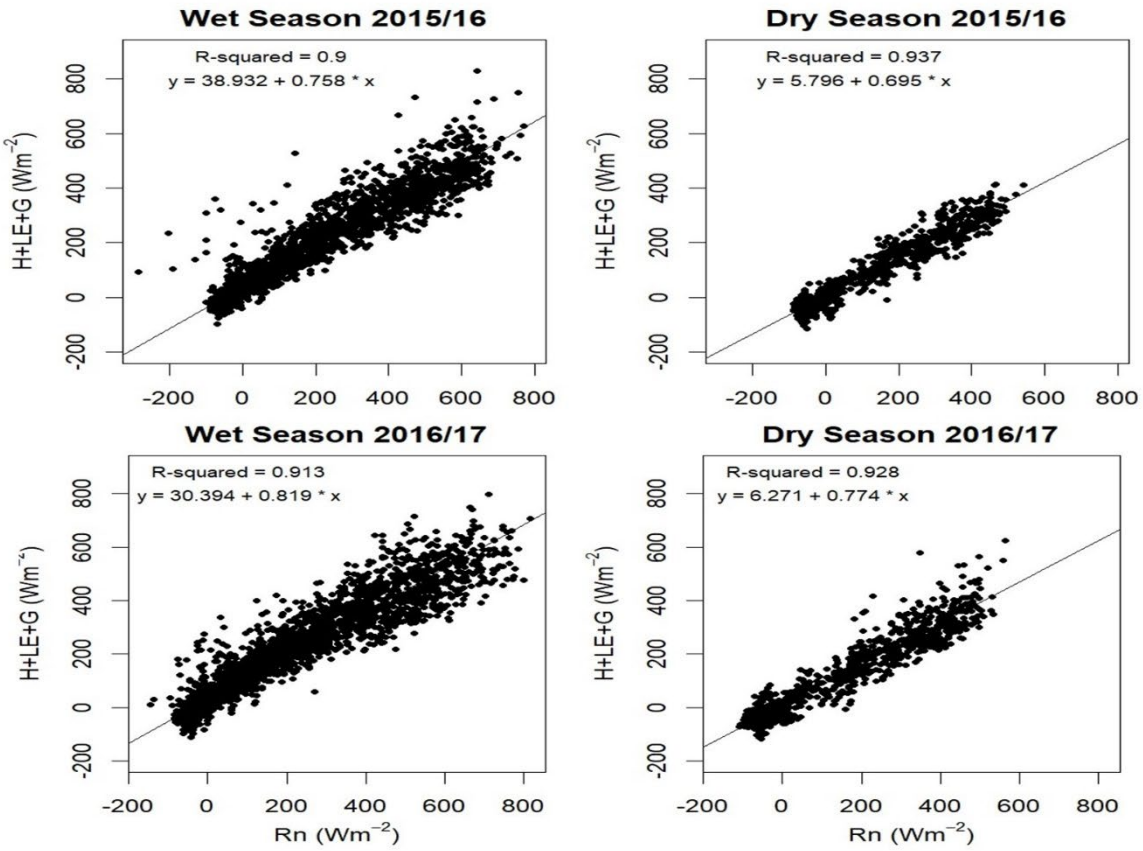

Figure 4.22. The energy closure for seasons 2015-2016, 2016-2017.

In Figure 4.22. there is a high positive correlation (r=0.9) between the two variables in the 2015–2016 wet season, and the regression equation shows that for every unit rise in Rn, H+LE+G increases by 0.758 units. The r-squared score of 0.9 indicates that this season's variance in Rn can account for 90% of the variation in H+LE+G. There is a significant positive correlation (r=0.937) between the two variables in the dry season of 2015–2016, and the regression equation shows that for every unit rise in Rn, H+LE+G increases by 0.695 units. The R-squared score of 0.937 indicates that this season's variance in Rn can account for 93.7% of the variation in H+LE+G. The regression equation shows that for each unit rises in Rn, H+LE+G increases by 0.819 units in the 2016–2017 wet season, indicating a high positive correlation between the two variables (r=0.913). The R-squared score of 0.913 indicates that this season's variance in Rn can account for 91.3% of the variation in H+LE+G.

There is a significant positive correlation (r=0.928) between the two variables in the dry season of 2016–2017, and the regression equation shows that for every unit rise in Rn, H+LE+G increases by 0.774 units. The R-squared score of 0.928 indicates that this season's variance in Rn can account for 92.8% of the variation in H+LE+G.

Table 4.3. Mean, Minimum, and Maximum Energy Fluxes by Time Scale

variable	timescale	Mean *(w/m²)*	Min *(w/m²)*	Max *(w/m²)*
H	30 min	57.364382	-99.854800	791.68050
H	hourly	57.981717	-97.872495	699.85275
H	daily	57.631191	-21.818418	192.77799
H	monthly	57.300458	27.586035	111.73484
LE	30 min	40.634973	-100.186630	598.58887
LE	hourly	41.131123	-89.087500	581.62402
LE	daily	41.819508	-13.349158	218.25352
LE	monthly	44.411374	3.897861	140.17394
Rn	30 min	120.399084	-421.500000	1060.50000
Rn	hourly	120.308692	-309.300000	1002.50000

The mean H values (57.30 to 57.98 w/m²) remain steady, reflecting consistent heat exchange between surface and atmosphere. Notably, larger variations emerge in 30-minute intervals, indicating rapid heat fluctuations. Mean LE values (40.63 to 44.41 w/m²) exhibit relative stability across timescales, mirroring consistent latent heat exchange. Similar to H, LE's min-max range is more variable in shorter intervals, suggesting swift moisture exchange changes. Rn indicates higher mean values (120.31 to 120.40 w/m²), implying continuous energy receipt/loss from the sun. Widening min-max range at shorter intervals underscores significant net energy balance variations due to solar radiation and heat loss shifts. Overall, longer timescales reveal steady heat/energy exchange, while shorter spans display more pronounced fluctuations.

Table 4.4. Fluxes and Energy Balances of Variable Measurements.

Variable	Turbulent Flux	Available Energy	Surface Energy Balance	NEE
NEE	Positive correlation	positive correlation	positive correlation with net radiation and soil heat flux	
Soil Moisture	Positive correlation at low soil moisture levels and positive correlation at high soil moisture levels	Directly proportional at low levels, inversely proportional at high levels	Positive correlation with net radiation and soil heat flux	Positive correlation at low soil moisture levels and positive correlation at high soil moisture levels
T_{air}	Positive correlation during the daytime and positive correlation during the nighttime	Directly proportional	Positive correlation with net radiation and soil heat flux	Positive correlation
RH	Positive correlation	Directly proportional	Positive correlation with net radiation and soil heat flux	Positive correlation
Tsoil	Positive correlation	Directly proportional	Positive correlation with net radiation and soil heat flux	Positive correlation
Rainfall	Positive correlation	Directly proportional	Positive correlation with net radiation and soil heat flux	Positive correlation

CHAPTER FIVE

5. CONCLUSION

Numerous energy and water fluxes impact the ecosystem under study and have varying effects on the NEE of carbon dioxide. In all four water years of data that were used, the link between NEE, LE, and Rn appears to have the strongest correlation. However, it appears that G and H have less impact on NEE. Rn and LE were discovered to be the most significant drivers of NEE in the water year 2010–2011. The association between NEE and G, Rn, H, and LE was generally poor in 2015–2016, although the positive correlation between NEE and H was somewhat more robust than the other fluxes. The dataset provides insight into the biometeorological and flow dynamics of the Skukuza ecosystem and how it responds to climate change.

Seasonal, monthly, daily energy fluxes, and NEE are affected by several environmental factors, including water availability, temperature, and solar radiation. The correlation between NEE and Rn is generally stronger during the wet seasons than during the dry seasons. Additionally, other environmental factors, such as soil moisture and temperature, also influence NEE during the dry season. Additionally, the ecosystem may function as a net carbon sink or source depending on prevailing conditions, such as the availability of sunlight and the dominance of photosynthesis or respiration. Therefore, it is essential to consider seasonality and climatic variability when studying the relationship between NEE and Rn to understand the complex interactions between ecosystem processes and environmental factors.

The energy closure principle emphasizes that the total energy entering or leaving an ecosystem must be balanced, and the energy balance equation should be satisfied within the ecosystem. The energy balance equation states that the sum of incoming and outgoing energy fluxes should be equal, i.e., the net radiation (Rn) equals the sum of sensible heat (H) and latent heat (LE) fluxes, as well as ground heat flux (G). The relationship between H+LE+G and Rn is influenced by the amount of annual precipitation, with a stronger relationship observed in wetter years. The relationship between H+LE+G and Rn-G is also positive, with a strong linear relationship observed in all four years studied. These findings highlight the importance of considering precipitation variability when studying the surface energy balance and its components.

Future work should focus on long-term monitoring to capture a wide range of climatic variability and its impacts on net ecosystem exchange (NEE). Advanced instrumentation should be employed to better measure ground heat flux (G) and sensible heat flux (H), as their roles in NEE are not fully understood. Detailed seasonal and spatial analyses are necessary to understand the drivers of NEE variability, particularly the differential impacts of net radiation (Rn), latent heat flux (LE), H, and G. Integrating observational data with ecosystem and climate models will help predict future changes in NEE and enhance understanding of ecosystem responses to climate change. Cross-site comparisons with similar ecosystems will help generalize findings and identify broader patterns in NEE and energy flux relationships.

REFERENCES

Archibald SA, A Kirton, M. van der Merwe, RJ Scholes, CA Williams, N Hanan (2008) Drivers of interannual variability in Net Ecosystem Exchange in a 1 semi-arid savanna ecosystem, South Africa, *Article in Biogeosciences · DOI: 10.5194/bgd-5-3221-2008.*

Aubinet, M., H. Berbigier, and T. Foken. (2000). "Long-term observations of the energy balance in a forest." *Agricultural and Forest Meteorology*, 104(1-3), 187-203. DOI: 10.1016/S0168-1923(00)00128-1

Aubinet M, Joly L, Loustau D (2016) Dimensioning IRGA gas sampling systems: laboratory and field experiments. *Atmos Meas Tech 9:1361–1367.*

Aubinet, M., T. Vesala, D. Papale (Eds.), (2012). Eddy Covariance: A Practical Guide to Measurement and Data Analysis. *Springer Atmospheric Sciences, Springer Verlag, 438.*

Aurela M., Lohila A., Tuovinen J.-P., Hatakka J., Penttilä T. & Laurila T. (2015): Carbon dioxide and energy flux measurements in four northern-boreal ecosystems at Pallas. *Boreal Env. Res. 20: 455–473.*

Baldocchi DD, Falge E, Wilson KW (2001a) A spectral analysis of biosphere-atmosphere trace gas flux densities and meteorological variables across hour to multi-year time scales. *Agricultural and Forest Meteorology, 10, 1–27.*

Baldocchi DD, Finnigan JJ, Wilson KW (2000) On measuring net ecosystem carbon exchange in complex terrain over tall vegetation. *Boundary Layer Meteorology, 96, 257–291.*

Baldocchi, D.D., Falge, E., Gu, L., et al. (2001). "FLUXNET: A New Tool to Study the Temporal and Spatial Variability of Ecosystem-Scale Carbon Dioxide, Water Vapor, and Energy Flux Densities." Bulletin of the American Meteorological Society, 82(11), 2415-2434.

Baldocchi, D., B. Hicks, and T. Meyers. (1988). Measuring biosphere-atmosphere exchanges of biologically related gases with micrometeorological methods. *Ecology 69, 1331-1340.*

Blackwell L., Lenschow DH, Mann J, Kristensen L (1994). How long is long enough when measuring fluxes and other turbulence statistics? *J Atmos Ocean Technol 11:661–673.*

Batchvarova E, Gryning S-E (1990) Applied model for the growth of the daytime mixed layer. *Boundary-Layer Meteorol 56:261–274.*

Behrendt A, Wulfmeyer V, Senff C (2019) Observation of sensible and latent heat flux profiles with lidar. *Atmos Meas Tech. https ://doi.org/10.5194/amt-2019- 305.*

Bombelli A, Henry M, Castaldi S, Adu-Bredu S, Arneth A, de Grandcourt A (*2009)* An outlook on the Sub-Saharan Africa carbon balance. *Biogeosciences.; 6(10):2193–205.*

Boussinesq J (1877) Essai sur la the´orie des eaux courantes. Mem Savants Etrange 23, 46 pp Bovscheverov VM, Voronov VP (1960) Akustitscheskii fljuger (Acoustic rotor). *Izv AN SSSR SerGeofiz 6:882–885.*

Budyko, M. I. (1974). Climate and Life. New York: *Academic Press. Google Scholar Biology, 2, 231-240.*

Burba, G. D. McDermitt, A. Grelle, D. Anderson, and L. Xu, (2008). Addressing the influence of instrument surface heat exchange on the measurements of CO_2 flux from open-path gas analyzers. *Global Change Biology, 14(8):1854-1876.*

Burba, G., (2013). Eddy Covariance Method for Scientific, Industrial, Agricultural and Regulatory Applications: A Field Book on Measuring Ecosystem Gas Exchange and Areal Emission Rates. *LI-COR Biosciences, Lincoln, USA, 33.*

Businger JA (1982) Equations and concepts. In: Nieuwstadt FTM, Van Dop H (eds) Atmospheric turbulence and air pollution modeling: *a course held in The Hague, 21–25 September 1981. D. Reidel Publ. Co., Dordrecht, 1–36.*

Businger JA, Oncley SP (1990) Flux measurement with conditional sampling. *J Atmos Ocean Technol 7:349–352.*

Blanford, J. R., J. G. B. A. Jensen, and B. A. Schaefer. (1991). "Large-scale non-turbulent transport processes in the energy balance." *Agricultural and Forest Meteorology*, 55(1-2), 109-123. DOI: 10.1016/0168-1923(91)90011-7

Bernhofer, C. (1992a). "Energy balance closure and turbulent transport processes." *Boundary-Layer Meteorology*, 59(1), 75-90. DOI: 10.1007/BF00123572

Council for Scientific and Industrial Research (CSIR). (n.d.) 'Eddy covariance flux towers', [Online]. Available at: https://www.csir.co.za/eddy-covariance-flux-towers (Accessed: 25 July 2024).

Canadell J, Mooney H, Baldocchi D (2000) Carbon metabolism of the terrestrial biosphere. *Ecosystems, 3, 115–130.*

Canadell J., Mooney H., Baldocchi D., Berry J., Ehleringer J., Field C.B., Gower T., Chapter 7 by Massman (pp. 133-158) in Lee, X., Massman, W, and Law, B.E., (2004). Handbook of micrometeorology. A guide for surface flux measurement and analysis. *Kluwer Academic Press, Dordrecht, 250.*

Charuchittipan D., Babel W., Mauder M., Leps J.P. and Foken T., (2014). Extension of the Averaging Time in Eddy-Covariance Measurements and Its Effect on the Energy Balance Closure. *Boundary-Layer Meteorology, 152(3): 303-327.*

Collins, M., R. Knutti, J. Arblaster, J.-L. Dufresne, T. Fichefet, P. Friedlingstein, X. Gao, W.J. Gutowski, T. Johns, G. Krinner, M. Shongwe, C. Tebaldi, A.J. Weaver, and M. Wehner, (2013): Long-term Climate Change: Projections, Commitments, and Irreversibility. *In: Climate Change, 233.*

Culf AD, Foken T, Gash JHC (2004) The energy balance closure problem. In: Kabat P, Claussen M (eds) Vegetation, water, humans, and the climate. *A new perspective on an interactive system. Springer, Berlin, 159–166.*

De Roo F., Zhang S., Huq S., and Mauder M. (2018). A semi-empirical model of the energy balance closure in the surface layer. *PLOS ONE, 13,12.*

De Vries DA (1963). Thermal Properties of Soils. In Physics of Plant Environment. Edited by VanWijk WR. Amsterdam: *North-Holland Publishing Company:210 – 235.*

Desjardins RL (1977) Description and evaluation of a sensible heat flux detector. *Bound Layer Meteorol 11:147–154.*

Desjardins RL (1991) Review of techniques to measure CO_2 flux densities from the surface and airborne sensors. *In: Advances in Bioclimatology (eds Stanhill G et al.), 2–23.*

Desjardins RL. (1974). A technique to measure CO_2 exchange under field conditions. *Int. J. Biometeorol. 18: 76-83.*

Desjardins RL (1985). Carbon dioxide budget of maize. *Agric. For. Meteorol.. 36: 29-41.*

Desjardins RL. (1991). Review of techniques to measure CO_2 flux densities from surface and airborne sensors. *Avd. Bioclimatol. G. Stanhill eds. Springer-Verlag. Berlin. 2-23.Ecosystems., 3, 115-130.*

Falge E, Baldocchi D, Olson R, Anthoni P, Aubinet M, Bernhofer C, Burba G, Ceulemans R, Clement R, Dolman H, Granier A, Gross P, Grunwald T, Hollinger D, Jensen NO, Katul G, Keronen P, Kowalski A, Lai CT, Law BE, Meyers T, Moncrieff H, Moors E, Munger JW, Pilegaard K, Rannik U, Rebmann C, Suyker A, Tenhunen J, Tu K, Verma S, Vesala T, Wilson K, Wofsy S (2001a) .Gap-filling strategies for long-term energy flux data sets. *Agric For Meteorol 107:71–77.*

Falge E, Baldocchi DD, Olson R (2001). Gap-filling strategies for defensible annual sums of net ecosystem exchange. *Agric. For. Meteorol.107, 43-69.*

Falge E., Baldocchi D., Tenhunen J., Aubinet M., Bakwin P., Berbigier P., Bernhofer C., Burba G., Clement R. & Davis K.J. (2002). Seasonality of ecosystem respiration and gross primary production as derived from FLUXNET measurements. *Agricultural and Forest Meteorology, 113, 53-74.*

Finnigan JJ, Clement R, Malhi Y (2003). A re-evaluation of long-term flux measurement techniques, part I: averaging and coordinate rotation. *Boundary-Layer Meteorol 107:1–48.*

Finnigan JJ. 1999 A comment on the paper by Lee (1998): "On micrometeorological observations of a surface-air exchange over tall vegetation", Agric. For. *Meteorol.97: 55-64.*

Foken T (1990) Probleme bei der Bestimmung vertikaler turbulenter Feuchtetransporte im Rahmen von ISLSCP-Experimenten (Ergebnisse von KUREX-88 und TARTEX-90). *In: Erste Deutsch-Deutsche Klimatagung. Berlin, 8.*

Foken T (1998) Die scheinbar ungeschlossene Energiebilanz am Erdboden - eine Herausforderung and die Experimentelle Meteorologie. *Sitzungsberichte der Leibniz-Sozietät 24:131–150.*

Foken T (2008(a)) Micrometeorology. *Springer, Berlin/Heidelberg, 308.*

Foken T (2008(b)) The energy balance closure problem: *an overview. Ecol Appl 18:1351–1367.*

Foken T, Aubinet M, Finnigan JJ (2011). Results of a panel discussion about the energy balance closure correction for trace gases. *Bull Am Meteorol Soc 92:ES13–ES18.*

Foken T, Buck AL, Nye RA, Horn RD (1998). A Lyman-alpha hygrometer with variable path length. *J Atmos Ocean Technol 15:211–214.*

Foken T, Falke H (2012) Technical note: calibration device for the krypton hygrometer KH20. *Atmos Meas Tech 5:1861–1867.*

Foken T, Gerstmann W, Richter SH et al (1993). Study of the energy exchange processes over different types of surfaces during TARTEX-90. *Dt Wetterd Forsch Entwicklung Arbeitsergebnisse 4:34.*

Foken T, Leuning R, Oncley, SP (2012) Corrections and data quality. In: Aubinet M, Vesala T, Papale D (eds) Eddy covariance: a practical guide to measurement and data analysis. *Springer, Dordrecht, pp 85–132.*

Foken T, Mauder M, Liebetha l C (2010) Energy balance closure for the LITFASS-2003 experiment. *Theor Appl Climatol 101:149–160.*

Foken Th, Wichura B. (1995). Tools for quality assessment of surface-based flux measurements, *Agric. For. Meteorol., 78, 83-105.*

Foken, T., W. Mauder, and H. S. Kerschgens. (1993). "A comprehensive study of energy balance closure in Tartu." *Agricultural and Forest Meteorology*, 63(3), 195-210. DOI: 10.1016/0168-1923(93)90056-6

Foken, T., M. Aubinet, and R. C. Oechel. (1998). "Energy balance closure in eddy covariance measurements: A case study in Kursk, Russia." *Boundary-Layer Meteorology*, 88(3), 243-257. DOI: 10.1023/A:1001821914147

Foken, T., W. Mauder, and J. W. M. H. Schuepp. (2004). "Some aspects of the energy balance closure problem." *Boundary-Layer Meteorology*, 113(3), 369-387. DOI: 10.1023/B.0000038203.84383.1c

Foken, T. (1990). "Problems with the energy balance closure in field experiments and their causes." *Boundary-Layer Meteorology*, 52(1), 23-30. DOI: 10.1007/BF00122464

Fuehrer, P.L., and Friehe, C.A. (2002). "Flux corrections revisited." Boundary-Layer Meteorology, 102(3), 415-457.

Finnigan, J.J., and Kaimal, J.C. (1994). "Atmospheric boundary layer flows: Their structure and measurement." Boundary-Layer Meteorology, 70(1), 3-34.

Friedlingstein, P (2019). Global Carbon Budget 2019. *Earth System Science Data, 11, 1783-1838.*

Fuehrer, P.L. and Friehe, C.A., (2002). Flux corrections revisited. *Boundary Layer Meteorology, 102:415-457.*

Goulden ML, Crill PM (1997). Automated measurements of CO_2 exchange at the moss surface of a black spruce forest. *Tree Physiology, 1Y, 537–542.*

Geider, R. J., E. H. Delucia (2001). "Primary productivity of planet earth: biological determinants and physical constraints in terrestrial and aquatic habitats." *Global Change Biology 7: 849-882.*

Gertenbach, W.P.D. (1980). Rainfall patterns in the Kruger National Park. *Koedoe. 23: 35 43.*

Gordon Bonan Cambridge University Press Print publication year:(2019) *Climate Change and Terrestrial Ecosystem Modeling, 101 – 114.*

Grünwald T, Bernhofer C (2007). A decade of carbon, water, and energy flux measurements of an old spruce forest at the Anchor Station Tharandt.*Tellus;59B:387–96.*

Horst, T.W., and Weil, J.C. (2003). "How far is far enough?: The fetch requirements for micrometeorological measurement of surface fluxes." Journal of Atmospheric and Oceanic Technology, 20(6), 836-856.
Horst TW, Weil JC (1994). How far is far enough?: The fetch requirements for micrometeorological measurement of surface fluxes. *J Atmos Ocean Technol 11:1018–1025.*

Jia, L.; Zheng, C.; Hu, G.C.; Menenti, M. (2018), "Evapotranspiration", *Comprehensive Remote Sensing, Elsevier, pp. 25–50.*

Jalota, S. K.; Vashisht, B. B.; Sharma, Sandeep; Kaur, Samanpreet (2018-01-01), Jalota, S. K.; Vashisht, B. B.; Sharma, Sandeep; Kaur, Samanpreet (eds.), "Chapter 1 - Emission of Greenhouse Gases and Their Warming Effect", Understanding Climate Change Impacts on Crop Productivity and Water Balance, *Academic Press, 1–53.*

Quansah, E., Mauder, M., Balogun, A.A., Amekudzi, L.K., Hingerl, L., Bliefernicht, J., & Kunstmann, H. (2015). Carbon dioxide fluxes from contrasting ecosystems in the Sudanian savanna in West Africa. *Carbon Balance and Management*, 10(1), 1-17. Available at: https://link.springer.com/article/10.1186/s13021-015-0040-2

Kowalski Andrew S. · Penélope Serrano-Ortiz (2007). On the relationship between the eddy covariance, the turbulent flux, and surface exchange for a trace gas such as CO_2. *Boundary-Layer Meteorol 124:129–141.*

Kaimal JC, Finnigan JJ (1994). The atmospheric boundary layer flows their structure and measurement. *Oxford University Press, Oxford, 289.*

Kanemasu, E. T., S. L. Yates, and G. N. Panin. (1992). "Energy balance closure in FIFE experiments." *Journal of Hydrology*, 138(1-4), 185-198. DOI: 10.1016/0022-1694(92)90032-L

Kirton, A.; Scholes, R.J.(2014). Site Characterization of the Malopeni Flux Tower Site, Kruger National Park, South Africa. Available online: Malopeni Site Characterisation.pdf (accessed on 1 April 2014).

Koitzsch, K., H. D. Maran, and A. A. Imasheva. (1988). "Energy balance in a savanna ecosystem in Australia." *Journal of Hydrology*, 104(1-2), 15-25. DOI: 10.1016/0022-1694(88)90003-4

Lee X (1998). On micrometeorological observations of surface-air exchange over tall vegetation. *Agric For Meteorol 91:39–49.*

Lee, X., W. Massman, and B. Law. (2004). Handbook of Micrometeorology. *Kluwer Academic Publishers, The Netherlands, 250.*

Lenschow DH (1995). Micrometeorological techniques for measuring biosphere–atmosphere trace gas exchange. *In: Biogenic Trace Gases: Measuring emissions from Soil and Water (eds Matson PA & Harriss RC), pp. 126–163.*

Leuning R (2007). The correct form of the Webb, Pearman, and Leuning equation for Eddy fluxes of trace gases in the steady and non-steady state, horizontally homogeneous flows. *Bound Layer Meteorol 123:263–267.*

Lee, X., and Massman, W. (2011). "A Perspective on Thirty Years of the Webb, Pearman and Leuning Density Corrections." Boundary-Layer Meteorology, 139(1), 37-59.

Lee, X., and Massman, W. (2012). "Density corrections for eddy covariance trace gas flux measurements." Agricultural and Forest Meteorology, 152, 223-236.

Liu, H. (2005). "An alternative approach for correcting the effects of heat and water vapor transport on the eddy covariance CO2 flux." Journal of Geophysical Research: Atmospheres, 110(D14).

Leuning, R. (2004). "Measurements of trace gas fluxes in the atmosphere using eddy covariance: WPL corrections revisited." Boundary-Layer Meteorology, 123(1), 177-187.

Leuning, R. (2007). "The correct form of the Webb, Pearman and Leuning (WPL) terms for trace gas fluxes: A comment." Boundary-Layer Meteorology, 123(1), 263-267.

Leuning RL, Moncrieff JB (1990). Eddy covariance CO2 flux measurements using open and closed path CO2 analyzers: correction for analyzer water vapour sensitivity and damping of fluctuations in air sampling tubes. *Bound Layer Meteorol 53:63–76.*

Leuning, R (2004). Measurements of trace gas fluxes in the atmosphere using eddy covariance: WPL corrections revisited, in Handbook of Micrometeorology: A Guide for Surface Flux Measurements and Analysis. *Kluwer, Dordrecht, 119–132.*

Leuning, R., G. B. Wilson, and M. D. P. Miller. (1982). "Comparison of eddy covariance and Bowen-ratio measurements of energy balance." *Agricultural and Forest Meteorology*, 27(3), 321-335. DOI: 10.1016/0168-1923(82)90045-6

Leuning, R., C. J. F. van Ginkel, and J. W. R. Hunt. (1988). "A new energy balance closure technique for the eddy covariance method." *Agricultural and Forest Meteorology*, 43(1-2), 133-145. DOI: 10.1016/0168-1923(88)90004-6

Li X, Liu L, Yang H, Li Y (2018). Relationships between carbon fluxes and environmental factors in a drip-irrigated, film-mulched cotton field in an arid region. *PLoS ONE 13(2): e0192467.*

Liang L.X., Shunlin; Li, Xiaowen; Wang, Jindi, eds. (2012-01-01), "Chapter 16 - Vegetation Production in Terrestrial Ecosystems", *Advanced Remote Sensing, Academic Press,501–531.*

Li-COR Inc., Lincoln Burba G, McDermitt DK, Grelle A, Anderson DJ, Xu L (2008). Addressing the influence of instrument surface heat exchange on the measurements of CO_2 flux from open-path gas analyzers. *Glob Chang Biol 14:1854–1876.*

Liebethal C, Huwe B, Foken T (2005). Sensitivity analysis for two ground heat flux calculation approaches. *Agric For Meteorol. 2005; 132:253–62.*

Liebethal, C. and Foken, T.: On the significance of the Webb correction to fluxes, Corrigendum, bound.-Lay.Meteorol.,113.

Liebethal, C., and Foken, T. (2003). "On the significance of the Webb correction to flux measurements." Boundary-Layer Meteorology, 109(1), 99-106.

Liebethal, C., and Foken, T. (2004). "Significance of the Webb correction for latent and sensible heat flux." Meteorologische Zeitschrift, 13(6), 489-494.

Lindsey, R. (2020). Climate and Earth's energy budget. *Accessed October 4, 2017.*

Liu H (2005). An Alternative Approach for CO_2 Flux Correction Caused by Heat and Water Vapour Transfer. *BLM,115, 151-168.*

Lloyd J, Taylor JA. On the temperature dependence of soil respiration. *FunctEcol. 1994; 8:315–23.*

Mauder M., T. Foken, R. Clement, J. A. Elbers, W. Eugster, T. Grunwald, B. Heusinkveld, and O. Kolle. (2007). Quality control of CarboEurope flux data – Part II: Inter-comparison of eddy-covariance software, *Biogeosciences Discuss., 4, 4067–4099.*

Mauder, M., and T. Foken. (2006). "Quality control of eddy covariance measurements." *Meteorologische Zeitschrift*, 15(1), 107-121. DOI: 10.1127/0941-2948/2006/0125

Mauder, M., and T. Foken. (2008). "The role of turbulent flux measurements in the energy balance closure problem." *Boundary-Layer Meteorology*, 126(2), 181-193. DOI: 10.1007/s10546-007-9212-0

Mauder, M., T. Foken, and B. E. Schmid. (2010). "Evaluation of eddy covariance flux data: Comparisons with other methods and closure problems." *Boundary-Layer Meteorology*, 136(2), 135-156. DOI: 10.1007/s10546-010-9470-7

Mauder M, Foken T(2011). Documentation and Instruction Manual of the Eddy-Covariance software Package TK3. *Arbeitsergebnisse 46, Bayreuth, Germany: Universität Bayreuth, Abteilung Mikrometeorologie,60.*

Mauder M, Liebethal C, Göckede M (2006). Processing and quality control of flux data during LITFASS-2003. *Boundary-Layer Meteorol, 121.*

Mauder M., Cuntz M., Drüe C., Graf A., Rebmann C., Schmid H.P., Schmidt M. and Steinbrecher R., (2013). A strategy for quality and uncertainty assessment of long-term eddy-covariance measurements. *Agricultural and Forest Meteorology, 169: 122-135.*
Meyers TP, Hollinger SE (2004). An assessment of storage terms in the surface energy balance of maize and soybean. *Agric For Meteorol 125:105–115.*

Massman, WJ, Lee X. (2002). Eddy covariance flux corrections and uncertainties in long-term studies of carbon and energy exchanges. *Agric. For. Meteorol.113, 121-144.*

Moncrieff, J. B. (2004). "Recent advances in eddy covariance research." *Agricultural and Forest Meteorology*, 125(1-2), 1-7. DOI: 10.1016/j.agrformet.2004.04.006

Moffat AM, Papale D, Reichstein M, Hollinger DY, Richardson AD, Barr AG, et al. Comprehensive comparison of gap-filling techniques for eddy covariance net carbon fluxes. *Agric For Meteorol. 2007; 147:209–32.*

Monteith John L.; Unsworth, Mike H. (2013-01-01), Monteith, John L.; Unsworth, Mike H. (eds.), "Chapter 16 - Micrometeorology: (i) Turbulent Transfer, Profiles, and Fluxes", Principles of Environmental Physics (Fourth Edition), *Academic Press, 289–320.*

Morales-Rincon LA, Hernandez AJ, Rodriguez-Hernandez NS and Jimenez R (2021). Carbon Exchange and Accumulation in an Orinoco High Plains Native Savanna Ecosystem as Measured by Eddy Covariance. Front. Environ. Sci. 9.

*Morales-Rincon, L.A., Hernandez, A.J., Rodriguez-Hernandez, N.S. and Jimenez, R. (2021) 'Carbon Exchange and Accumulation in an Orinoco High Plains Native Savanna Ecosystem as Measured by Eddy Covariance', *Frontiers in Environmental Science*, 9. Available at: https://doi.org/10.3389/fenvs.2021.673932 (Accessed: 25 July 2024).*

Nickless, A., Archibald, S., Van der Merwe, M.R., Scholes, R., Williams, C., & Hanan, N. (2011) 'Estimation of net ecosystem exchange at the Skukuza flux site, Kruger National Park, South Africa', *Africa and the Carbon Cycle: Proceedings of the Open Science Conference on "Africa and Carbon Cycle: the CarboAfrica project"*, Accra, Ghana, 25-27 November 2008. Available at: http://hdl.handle.net/10204/5135 (Accessed: 25 July 2024).

Oncley SP, Businger JA, Itsweire EC (1990). Surface layer profiles and turbulence measurements over uniform land under near-neutral conditions. In: 9th Symposium on boundary layer and turbulence. *American Meteorological Society, Roskilde, Denmark, 237–240.*

Oncley SP, Foken T, Vogt R (2007). The energy balance experiment EBEX-2000. Part I: overview and energy balance. *Boundary-Layer Meteorol 123:1–28.*

Panin GN, Bernhofer C (2008). Parametrization of turbulent fluxes over inhomogeneous landscapes. *Izv Atmos Ocean Phys 44:701–716*.

Panin GN, Raabe A, Tetzlaf G (1998). Inhomogeneity of the land surface and problems in the parametrization of surface fluxes in natural conditions. *Theor Appl Climatol 60:163–178.*

Penman, H. L. (1948). Natural evaporation from open water, bare soil, and grass. *Proceedings of the Royal Society of London, 193A, 120–145.*

Richardson AD, Aubinet M, Barr AG (2012). Uncertainty quantification. In: Aubinet M, Vesala T, Papale D (eds) Eddy covariance: a practical guide to measurement and data analysis. *Springer, Dordrecht, 173–210.*

Running SW, Baldocchi DD, Turner D, Gower ST, Bakwin P, Hibbard K. (1999). A global terrestrial monitoring network, scaling tower fluxes with ecosystem Modeling and EOS satellite data. *Rem. Sen. Environ. 70, 108-127.*

Reichstein, M., Falge, E., Baldocchi, D. et al. (2005). "On the separation of net ecosystem exchange into assimilation and ecosystem respiration: review and improved algorithm." Global Change Biology, 11, 1424-1439.

Ramoelo, A., Cho, M. A., van Aardt, J. A., & Mathieu, R. (2014). *Evaluation of MOD16 evapotranspiration estimates over South Africa using eddy covariance measurements*. *Remote Sensing*, 6(10), 9784-9807. https://doi.org/10.3390/rs6109784

Schlesinger William H.; Bernhardt Emily S. (2013-01-01), Schlesinger, William H.; Bernhardt, Emily S. (eds.), "Chapter 7 - Wetland Ecosystems", Biogeochemistry (Third Edition), *Academic Press, 233–274.*

Schmid HP (1994). Source areas for scalars and scalar fluxes. *Boundary Layer Meteorology, 293–318.*

Scholes, M. C., Scholes, R. J., Otter, L. B., and Woghiren, A. J (2004).: Biogeochemistry: the cycling of elements, in The Kruger Experience: ecology and management of savanna heterogeneity. *Island Press, Washington DC, 130-148.*

Scholes, R.; Gureja, N.; Giannecchinni, M.; Dovie, D.; Wilson, B.; Davidson, N.; Piggot, K.; McLoughlin, C.; van der Velde, K.; Freeman, A.; et al. (2001). The environment and vegetation of the flux measurement site near Skukuza, Kruger National Park. *Koedoe, 44, 73–83.*

Shea, R. W., Shea, B. W., Kaufman, J. B., Ward, D. E., Haskins, C. I., and Scholes, M. C. (1996). Fuel mass and combustion factors associated with fires in savanna ecosystems of South Africa and Zambia, *Journal of Geophysical Research, 23551-23568.*

Shotanus P, Nieuwstadt FTM, De Bruin HAR(1983). Temperature measurement with a sonic anemometer and its application to heat and moisture fluxes. *Bound-Layer Meteorol; 26:81–93.*

Stoy P.C (2013). A data-driven analysis of energy balance closure across FLUXNET research sites: The role of landscape-scale heterogeneity. *Agricultural and Forest Meteorology, 171-172: 137–152.*

Stull, R. B (1988). An Introduction to Boundary Layer Meteorology, *Kluwer, Dordrecht, 666.*

Twine TE, Kustas WP, Norman JM (2000). Correcting eddy-covariance flux underestimates over a grassland. *Agric For Meteorol 103:279–300.*

Twine, T. E., S. M. E. McDermitt, and A. B. A. Chen. (2000). "Adjusting for general flow measurements in energy balance studies." *Boundary-Layer Meteorology*, 96(3), 273-295. DOI: 10.1023/A:1001774829053

Tyson PD, Dyer TG, Mametse MN(1975). Security changes in South African rainfall: 1880 to 1972. *Quarterly Journal of Royal Meteorological Society; 101, 817-833.*

Tsvang, A., L. A. Kasatkin, and A. V. Vorobiev. (1991). "Energy balance closure studies in the Tartu experiment." *Agricultural and Forest Meteorology*, 53(3), 237-250. DOI: 10.1016/0168-1923(91)90011-3

Verma SB (1990). Micrometeorological methods for measuring surface fluxes of mass and energy. *Remote Sensing Reviews, 5, 99–115.*

Webb EK, Pearman GI, Leuning R (1980). Correction of the flux measurements for density effects due to heat and water vapour transfer. *Quart J Roy Meteorol Soc; 106:85–100.*

Webb, E.K., Pearman, G.I., and Leuning, R. (1980). "Correction of flux measurements for density effects due to heat and water vapour transfer." Quarterly Journal of the Royal Meteorological Society, 106(447), 85-100.

Wilczak JM, Oncley SP, Stage SA.(2001). Sonic anemometer tilt correction algorithms. *Bound-Layer Meteor; 99:127–50.*

Wilson K, Goldstein A, Falge E (2002). Energy balance closure at FLUXNET sites. *Agric For Meteorol 113:223–243.*

Wilson, K. B., R. M. M. Grant, and S. E. M. Haggerty. (2002). "Evaluating energy balance closure in eddy covariance measurements." *Agricultural and Forest Meteorology*, 112(1-2), 39-58. DOI: 10.1016/S0168-1923(02)00068-5

Wofsy SC, Goulden ML, Munger JW, Fan SM, Bakwin PS (1993). Net exchange of CO_2 in a mid-latitude forest, *Science. 260: 1314-1317.*

Zhang Y, Liu H, Foken T (2010). *Turbulence spectra and cospectra under the influence of large eddies in the energy balance experiment (EBEX). Boundary-Layer Meteorol 136:235–251.*